Molecular Phylogenetics and Evolution 164 (2021) 107212

Contents lists available at ScienceDirect

Molecular Phylogenetics and Evolution

journal homepage: www.elsevier.com/locate/ympev

Dated phylogeny and ancestral range estimation of sand scorpions (Buthidae: *Buthacus*) reveal Early Miocene divergence across land bridges connecting Africa and Asia

Shlomo Cain [a], Stephanie F. Loria [b], Rachel Ben-Shlomo [c], Lorenzo Prendini [b], Eran Gefen [c,*]

[a] Department of Evolutionary and Environmental Biology, Faculty of Natural Sciences, University of Haifa, Israel
[b] Scorpion Systematics Research Group, Arachnology Lab, Division of Invertebrate Zoology, American Museum of Natural History, New York, USA
[c] Department of Biology and Environment, Faculty of Natural Sciences, University of Haifa – Oranim, Israel

ARTICLE INFO

Keywords:
Chelicerata
Scorpiones
Buthidae
Systematics
Phylogeny
Biogeography

ABSTRACT

Sand scorpions of the genus *Buthacus* Birula, 1908 (Buthidae C.L. Koch, 1837) are widespread in the sandy deserts of the Palearctic region, occurring from the Atlantic coast of West Africa across the Sahara, and throughout the Middle East to Central Asia. The limits of *Buthacus*, its two species groups, and many of its species remain unclear, and in need of revision using modern systematic methods. The study presented here set out to investigate the phylogeny and biogeography of the *Buthacus* species occurring in the Levant, last studied in 1980. A phylogenetic analysis was performed on 104 terminals, including six species collected from more than thirty localities in Israel and other countries in the region. Three mitochondrial and two nuclear gene loci were sequenced for a total of 2218 aligned base-pairs. Morphological datasets comprising 22 qualitative and 48 quantitative morphological characters were compiled. Molecular and morphological datasets were analyzed separately and simultaneously with Bayesian Inference, Maximum Likelihood, and parsimony. Divergence time and ancestral range estimation analyses were performed, to understand dispersal and diversification. The results support a revised classification of Levantine *Buthacus*, and invalidate the traditional species groups of *Buthacus*, instead recovering two geographically-delimited clades, an African clade and an Asian clade, approximately separated by the Jordan Valley (the Jordan Rift Valley or Syro-African Depression), the northernmost part of the Great Rift Valley. The divergence between these clades occurred in the Early Miocene (ca. 19 Ma) in the Levant, coinciding temporally with the existence of two land bridges, which allowed faunal exchange between Africa and Asia.

1. Introduction

Scorpions of the genus *Buthacus* Birula, 1908 (Buthidae C.L. Koch, 1837), commonly known as 'sand scorpions', are widespread in the sandy deserts of the Palearctic region, from the Atlantic coast of West Africa across the Sahara, and throughout the Middle East to Central Asia (Vachon, 1952; Levy et al., 1973; Levy and Amitai, 1980; Fet and Lowe, 2000; Lourenço, 2004; Lourenço and Qi, 2006; Yağmur et al., 2008; Zambre and Lourenço, 2010). All species of the genus possess a suite of ultrapsammophilous to semi-psammophilous adaptations for locomotion and burrowing on sandy substrates (Cain et al., 2021). Stenotopic specialization to sandy substrates and homing behavior, considered adaptive in burrowing species (Polis et al., 1986), may have limited the vagility of *Buthacus* and, together with the fragmented nature of sandy habitats, disrupted gene flow between isolated populations, promoting speciation by vicariance in the genus (Prendini, 2001a).

Although many new species of *Buthacus* were described in recent years, no modern revision exists for the genus, and the limits of many infrageneric taxa remain unclear. The present contribution addresses the phylogeny of *Buthacus* species recorded from the Levant, defined here as the region of the Middle East including Syria, Lebanon, Jordan, Israel, the Palestinian territories and the Sinai Peninsula of Egypt. The scorpion fauna of this region was well studied by Levy et al. (1973) and Levy and Amitai (1980) who recognized four species and subspecies of *Buthacus* in Israel and the Sinai Peninsula, based on morphological characters (Fig. 1). *Buthacus leptochelys nitzani* Levy et al., 1973, endemic to the

* Corresponding author.
E-mail address: gefene@research.haifa.ac.il (E. Gefen).

https://doi.org/10.1016/j.ympev.2021.107212
Received 17 December 2020; Received in revised form 10 May 2021; Accepted 19 May 2021
Available online 23 May 2021

Haluza sand dunes in the northern Negev Desert, was described as a distinct subspecies from the more widely distributed nominotypical form of *Buthacus leptochelys* (Ehrenberg, 1829), *Buthacus yotvatensis* Levy et al., 1973 was described from the southern part of the Jordan Valley (the Arava Valley), and specimens from northern Sinai were identified as *Buthacus arenicola* (Simon, 1885) (Fig. 1). Levy and Amitai (1980), followed by others (e.g., Lourenço, 2006), doubted whether the population of *B. arenicola* occurring east of Libya was conspecific with the typical population, to the west. Levy et al. (1973) also considered placing *B. yotvatensis* in a different genus. However, following Vachon (1952), Levy et al. (1973) and Levy and Amitai (1980) proposed dividing the species of *Buthacus* into two groups, the *B. arenicola* group and the *B. leptochelys* group, based on the dentition of the movable finger of the pedipalp chela. Lourenço (2006) observed significant variation in finger dentition and questioned its utility for species assignment to the two groups, but the character remained in widespread use for species diagnosis in the genus (Kovařík, 2005, 2018; Lourenço, 2006; Zambre and Lourenço, 2010; Lourenço and Sadine, 2015; Kovařík et al., 2016; Alqahtani and Badry, 2020).

Various updates to the systematics of Levantine *Buthacus* were provided subsequently (Vachon and Kinzelbach, 1987; El-Hennawy, 1987, 1992; Amr et al., 1988, 2015; Amr and El-Oran, 1994; Kabakibi et al., 1999; Kovařík, 2001, 2005; Kovarik and Whitman, 2004; Lourenço, 2006; Shehab et al., 2011; Amr, 2015; Saleh et al., 2017; Badry et al., 2018; Lowe et al., 2019) such that, prior to Cain et al. (2021), five infrageneric taxa of *Buthacus*, including several synonyms, were recognized from the region. Based on extensive new collections and a reassessment of the morphology (including multivariate statistical analysis),

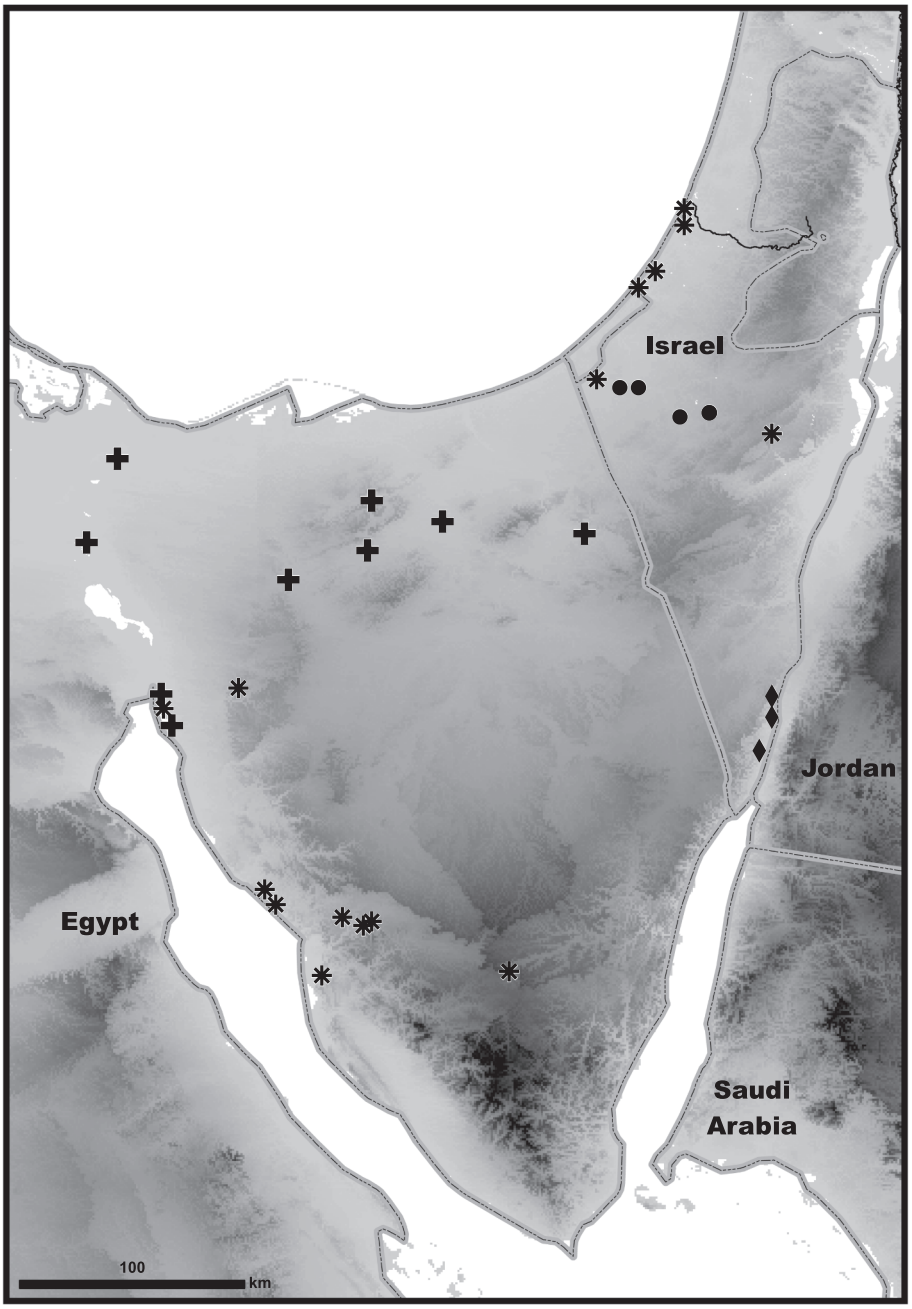

Fig. 1. Records of sand scorpions, genus *Buthacus* Birula, 1908 (Buthidae C.L. Koch, 1837) in Israel and Sinai, after Levy and Amitai (1980). ✱ *Buthacus l. leptochelys* (Ehrenberg, 1828); ● *Buthacus leptochelys nitzani* Levy et al., 1973; ✚ *Buthacus arenicola* (Simon, 1885); ◆ *Buthacus yotvatensis* Levy et al., 1973.

Cain et al. (2021) elevated *Buthacus nitzani* Levy et al., 1973 to the rank of species and described three new species, *Buthacus amitaii* Cain et al., 2021, *Buthacus arava* Cain et al., 2021, and *Buthacus levyi* Cain et al., 2021, raising the number of *Buthacus* species in the Levant, to seven.

The present contribution set out to test the monophyly of the *B. arenicola* and *B. leptochelys* species groups, and reconstruct the phylogenetic relationships and biogeographical history of *Buthacus* in the Levant, in light of geological events associated with plate tectonics, which provide the backdrop for biotic diversification in the region (Leprieur et al., 2016; Ficetola et al., 2017; Zaffos et al., 2017; Pellissier et al., 2018). The rich biodiversity of the Levant has been attributed to its position at the crossroads of Africa and Asia over the course of its geological history (Tchernov, 1988) but studies on the biogeography of its arthropods remain scarce. A recent phylogenetic analysis based on seven 16S rDNA sequences, representing three species of *Buthacus* (Alqahtani and Badry, 2020), recovered a clade comprising two African species, *B. arenicola* and *B. leptochelys*, to the exclusion of an Asian species, *Buthacus nigroaculeatus* Levy et al., 1973. This hypothesis is tested here with phylogenetic analyses of a more extensive dataset, comprising DNA sequence data from two nuclear and three mitochondrial gene loci and morphological characters for 103 ingroup terminals, including six species collected from more than thirty localities across the region, as well as divergence time and ancestral range estimation analyses on a reduced molecular dataset including one terminal per species.

The results support the classification of Levantine *Buthacus* by Cain et al. (2021), and invalidate the traditional species groups of *Buthacus*, instead recovering two geographically-delimited clades, an African clade and an Asian clade, approximately separated by the Jordan Valley (the Jordan Rift Valley or Syro-African Depression), the northernmost part of the Great Rift Valley. The divergence between these clades occurred in the Early Miocene (ca. 19 Ma) in the Levant, coinciding temporally with the existence of two land bridges, which allowed faunal exchange between Africa and Asia.

2. Materials and methods

2.1. Fieldwork and material

Specimens were collected from type localities and other suitable habitat with ultraviolet (UV) light detection (Stahnke, 1972) using portable UV-LED lamps on warm, dark nights, around the new moon. Material was preserved in 80% ethanol for morphological study, and 96% ethanol for DNA isolation. Additional material was donated by citizen scientists.

Material is deposited in the American Museum of Natural History, New York (AMNH), with tissue samples stored at −20 °C in the Ambrose Monell Cryocollection (AMCC), and the National Natural History Collection at the Hebrew University of Jerusalem, Israel (HUJ).

2.2. Taxon sampling

The dataset comprised 103 ingroup taxa representing 33 localities in Israel, Egypt and Tunisia (Table 1). Material sampled at sites 1–9 and 13–15 (Table 1; Fig. 2C) corresponds to the two subspecies of

Table 1
Collection locality data for samples used in phylogenetic analysis of sand scorpions, genus *Buthacus* Birula, 1908 (Buthidae C.L. Koch, 1837): *Buthacus amitaii* Cain et al., 2021, *Buthacus arava* Cain et al., 2021; *Buthacus arenicola* (Simon, 1885); *Buthacus leptochelys* (Ehrenberg, 1828); *Buthacus levyi* Cain et al., 2021; *Buthacus nitzani* Levy et al., 1973; *Buthacus yotvatensis* Levy et al., 1973; and an outgroup taxon, *Androctonus amoreuxi* (Linneaus, 1758).

Species	Site	Country: Locality	Georeference	*N*	Species	Site	Country: Locality	Georeference	*N*
B. nitzani	1	Israel: Palmahim	31°54′39.4″N 34°43′31.8″E	2	*B. levyi*	9	Israel: Be'er Milka, Holot Haluza sand dunes	30°55′42.5″N 34°24′41.9″E	7
	2	Israel: Ashdod	31°48′53.5″N 34°39′11.3″E	2		19	Egypt		2
	3	Israel: The Great Dune, Ashdod Nizzanim Nat. Res.	31°46′18.3″N 34°39′09.7″E	3		20	Egypt: Qesm Remanah	30°59′39.1″N 32°46′17.9″E	1
	4	Israel: Nizzanim, Ashdod Nizzanim Nat. Res.	31°45′16.0″N 34°38′06.8″E	7		21	Egypt: Qesm Ad Dabaah	31°02′34.7″N 28°26′37.2″E	1
	5	Israel: Ashqelon	31°37′50.7″N 34°32′46.3″E	2		22	Egypt: Qesm Ad Dabaah	30°58′40.1″N 28°28′33.6″E	1
	6	Israel: Retamim, Holot Haluza sand dunes	31°04′16.5″N 34°41′55.1″E	8		23	Egypt: Abou Rawash	30°02′32.3″N 31°05′10.2″E	1
	7	Israel: Mashabbim, Holot Haluza sand dunes	31°05′00.8″N 34°41′11.0″E	1	*B. arava*	24	Israel: Nahal Sha'alav	30°02′40.6″N 35°06′33.7″E	1
	8	Israel: Ramat Hovav, Holot Haluza sand dunes	31°05′32.7″N 34°49′01.6″E	3		25	Israel: Lotan	30°00′10.4″N 35°05′44.1″E	5
	9	Israel: Be'er Milka, Holot Haluza sand dunes	30°55′42.5″N 34°24′41.9″E	5		26	Israel: Yotvata	29°53′21.1″N 35°04′34.8″E	2
B. leptochelys	10	Egypt: Zafarana	29°04′36.3″N 32°27′07.9″E	1	*B. yotvatensis*	27	Israel: Nahal Gidron	30°46′52.2″N 35°14′33.5″E	1
	11	Egypt: Zafarana	29°04′22.0″N 32°26′48.9″E	1		28	Israel: Nahal Mashaq	30°47′26.1″N 35°15′26.5″E	1
	12	Egypt: Faiyum Oasis	29°32′11.0″N 30°48′08.8″E	1		29	Israel: Nahal Shezaf	30°44′36.0″N 35°16′03.2″E	1
B. amitaii	13	Israel: Mamshit	31°01′50.7″N 35°04′35.2″E	6		30	Israel: Ein Zik campsite	30°48′22.4″N 34°51′03.1″E	2
	14	Israel: Nahal Yamin	30°57′01.8″N 35°04′51.7″E	4		24	Israel: Nahal Sha'alav	30°02′40.6″N 35°06′33.7″E	2
	15	Israel: Color Sands, Ha-Makhtesh Ha-Gadol	30°57′07.9″N 35°01′34.9″E	5		25	Israel: Lotan	30°00′10.4″N 35°05′44.1″E	2
B. arenicola	16	Tunisia: Tozeur	33°56′35.3″N 07°50′13.7″E	1		31	Israel: Hay-Bar Yotvata Nat. Res.	29°50′51.0″N 35°01′42.5″E	6
	17	Tunisia: Tozeur	33°56′22.0″N 07°50′19.3″E	1		32	Israel: Samar sand dunes	29°49′36.8″N 35°02′35.8″E	7
	18	Tunisia: Tozeur	33°51′12.5″N 07°44′00.7″E	1		33	Israel: Avrona Nature Reserve	29°41′12.5″N 34°59′46.2″E	6
					A. amoreuxi	9	Israel: Be'er Milka, Holot Haluza sand dunes	30°55′42.5″N 34°24′41.9″E	1

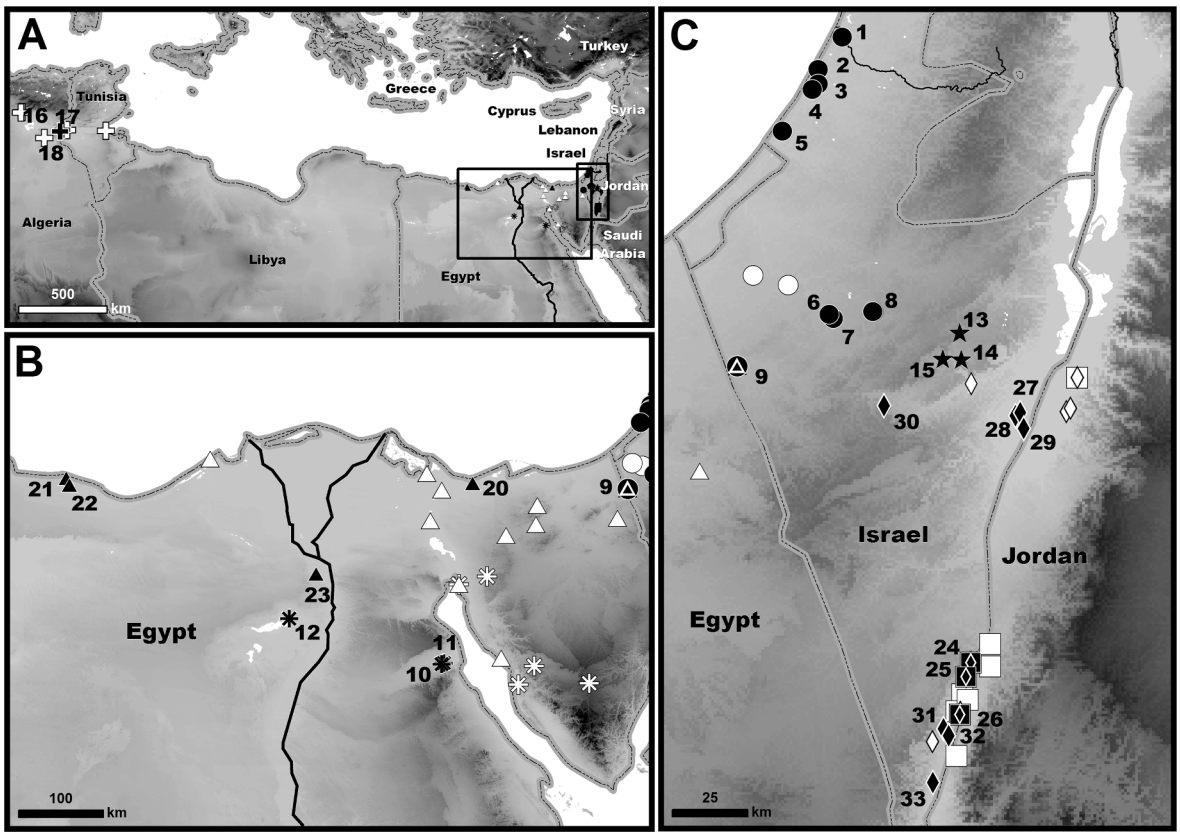

Fig. 2. Collection localities of sand scorpions, genus *Buthacus* Birula, 1908 (Buthidae C.L. Koch, 1837) in Tunisia (**A**), Egypt, Israel and Jordan (**B, C**). Black symbols indicate localities from which specimens were sequenced for the phylogenetic analysis, whereas white symbols represent localities from which specimens were only examined morphologically. ★ *Buthacus amitaii* Cain et al., 2021; ■ *Buthacus arava* Cain et al., 2021; ✚ *Buthacus arenicola* (Simon, 1885); ✱ *Buthacus leptochelys* (Ehrenberg, 1828); ▲ *Buthacus levyi* Cain et al., 2021; ● *Buthacus nitzani* Levy et al., 1973; ◆ *Buthacus yotvatensis* Levy et al., 1973. *Buthacus arava* and *B. yotvatensis* were sympatric at sites 24–26, whereas *B. levyi* and *B. nitzani* were sympatric at site 9. See Table 1 for locality data.

B. leptochelys occurring in Israel, as reported by Levy and Amitai (1980), with sites 6 and 7 (Table 1, Fig. 2C) situated near the type locality of *B. nitzani*. Samples from three localities (sites 10–12) in mainland Egypt, east and west of the Nile River (Table 1; Fig. 2B), correspond to the nominotypical form of *B. leptochelys*, described from Egypt (Cain et al., 2021).

As *B. arenicola* was reported to occur in Sinai by Levy and Amitai (1980), sandy habitats near Be'er Milka (site 9 in Fig. 2C) were thoroughly surveyed. These efforts yielded material that was morphologically indistinguishable from material collected in northern Sinai and previously identified as *B. arenicola* by Levy and Amitai (1980). However, the Be'er Milka material was morphologically distinct from material collected near the type locality of *B. arenicola* in Tunisia, supporting the opinions of Levy and Amitai (1980) and Lourenço (2006) that specimens previously assigned to *B. arenicola* from localities to the east of Libya are not conspecific with *B. arenicola* (discussed further by Cain et al. (2021), who described these populations as *B. levyi*). In order to test this hypothesis with phylogenetic analysis, specimens from the vicinity of Tozeur, Tunisia, the type locality of *B. arenicola* (Table 1, Fig. 2A; sites 16–18), and four localities (sites 20–23) in the Sinai Peninsula and mainland Egypt, west of the Nile River (Table 1; Fig. 2B), were included, along with two Egyptian specimens acquired from a dealer, for which precise locality data were unavailable (Table 1).

As published phylogenetic analyses of Buthidae are partial and conflicting (Fet et al., 2003; Suranse et al., 2017), *Androctonus amoreuxi* (Linneaus, 1758) was selected as outgroup based on a preliminary analysis of the five concatenated gene loci used in this study (see below), in which it was placed closer to *Buthacus* than the other two buthid outgroup species included, *Buthus israelis* Shulov and Amitai, 1959 and *Hottentotta judaicus* (Simon, 1872).

2.3. DNA sequencing

DNA isolation, PCR amplification and sequencing were conducted at the University of Haifa – Oranim and the AMNH Sackler Institute for Comparative Genomics, using standard protocols (Prendini et al., 2002, 2003, 2005) and primers (Supplementary Table S1).

A multilocus dataset was produced for the 103 ingroup terminals and one outgroup terminal from five gene loci, which provide different levels of phylogenetic resolution and were selected based on previous studies of scorpions and other arachnids (Prendini et al., 2003, 2005; Bryson et al., 2013a): 277 base-pairs (bp) of the 12S rDNA (12S), 269 bp of the 16S rDNA (16S) and 616 bp of the Cytochrome *c* Oxidase Subunit I (COI), from the mitochondrial genome; and 510 bp of the D3 region of the 28S rDNA (28S) and 480 bp of the Internal Transcribed Spacer 2 (ITS2) from the nuclear genome.

Genomic DNA was extracted from leg muscle tissue using the DNeasy 96 Blood and Tissue Kit (Qiagen, Hilden, Germany). DNA was amplified using GoTaq® Green Master Mix (Promega, Maddison, WI, U.S.A.), 1 µl (10 µM) of each primer, and 1–4 µl of DNA template. The PCR program involved an initial denaturing step at 94 °C for 5 min, 40 amplification cycles (94 °C for 15 s, 50 °C for 10 s, 72 °C for 15 s), and a final step of 72 °C for 7 min, in a GeneAmp PCR System 9700 thermocycler (Applied Biosystems, Foster City, CA, U.S.A.). Specific conditions were optimized for samples or primer pairs (e.g., a lower annealing temperature was used for COI). PCR products were verified on 1–1.5% agarose-TBE gels and purified with QIAquick columns (Qiagen), illustra™ ExoProstar™ (GE Healthcare Life Sciences, Little Chalfont, U.K.), or AMPure Magnetic

Table 2
Genomic data statistics for aligned DNA sequences of two nuclear and three mitochondrial gene markers used for phylogenetic analysis of sand scorpions, genus *Buthacus* Birula, 1908 (Buthidae C.L. Koch, 1837): aligned length (base-pairs); model selected by Akaike Information Criterion (AIC); number and percentage of variable positions; number and percentage of parsimony-informative (PI) positions, including gaps (and percentage of aligned length); mean percentage nucleotide composition; percentage of transitions (ts) and transversions (tv) for each nucleotide combination and overall. Calculations were conducted using the maximum composite likelihood test (mcl) under the Tamura et al. (2004) model of substitution.

		Nuclear		Mitochondrial			
		ribosomal 28S	ITS2	12S	16S	protein-coding COI	Total
Length (bp)		510	541	281	270	616	2218
AIC		HKY + I	K80 + I	HKY + G	GTR + G	GTR + I	-
Variable (%)		17 (3)	159 (29)	95 (34)	88 (33)	159 (26)	518 (23)
PI (%)		9 (2)	79 (15)	74 (26)	74 (27)	129 (21)	365 (16)
	A	24	22	40	38	42	33
	C	26	28	8	9	25	22
	G	31	25	19	18	13	21
	T	19	24	33	35	20	24
ts	A → G	27.92	24.23	18.17	23.24	0.59	11.45
	G → A	20.75	21.19	38.98	50.1	1.98	17.85
	T → C	10.39	12.16	6.78	2.64	43.52	16.52
	C → T	7.55	10.11	28.44	9.97	34.23	18.49
tv	A/G → T	3.17	3.84	1.26	2.43	1.98	4.34
	A/G → C	4.37	4.61	0.3	0.64	2.51	3.88
	T/C → A	3.9	3.6	1.54	2.7	4.12	5.87
	T/C → G	5.25	4.11	0.72	1.25	1.24	3.76
ts: tv		2.23	2.24	1.12	4.53	0.03	0.71

Beads Purification System (Beckman Coulter, Brea, CA, U.S.A.), followed by Sanger dideoxy sequencing using an ABI 3730 automated sequencer (Applied Biosystems). The accuracy of sequences was verified by independently amplifying and sequencing the complementary strands of all fragments. Primer sequences were removed and complementary strands of DNA assembled into consensus sequences, edited, and checked for quality using MEGA6 (Tamura et al., 2013), and Sequencher ver. 5.4.6 (Gene Codes, Ann Arbor, MI, U.S.A.). If complementary strands disagreed (besides minor mismatches), the sample was reamplified and sequenced to resolve discrepancies. Edited contig sequences are deposited in GenBank (https://www.ncbi.nlm.nih.gov/genbank; Supplementary Table S2).

Sequence length was calculated using the script "gc_calculator.py" in Biopython (Cock et al., 2009). Due to missing data, sequence length was variable across all loci: 12S: 246–277 bp; 16S: 238–269 bp; COI: 266–616 bp, 28S: 186–510 bp, ITS2: 318–480 bp. Sequences of the 12S, 16S and ITS2 loci were mostly complete for all terminals. Two terminals, *B. amitaii* (HUJ INVSC 3472) and *B. levyi* (AMCC [LP 16601]), were missing 256 and 351 bp, respectively, of the COI locus and five terminals, *B. leptochelys* (AMCC [LP 16599, 16600]), *B. amitaii* (HUJ INVSC 3474), *B. yotvatensis* (HUJ INVSC 3482) and *B. levyi* (AMCC [LP 16587]) were missing 190, 193, 209, 221 and 325 bp, respectively, of the 28S locus.

2.4. Morphological data

A morphological data matrix, comprising 22 qualitative characters (Supplementary Table S3) was prepared using WinClada v. 1.00.08 (Nixon, 2002). Characters scored in the matrix included traits capturing the morphological diversity within *Buthacus*, most pertaining to the adult stage: total length, 1 (5%); pedipalps, 6 (27%); legs, 1 (5%); pectines, 4 (18%); metasoma, 6 (27%); telson, 4 (18%). Morphological terminology follows previous phylogenetic analyses of Buthidae by one of the authors (e.g., Prendini, 2001b, 2004; Prendini and Esposito, 2010; Esposito et al., 2018). Four multistate characters were treated as unordered/non-additive (Fitch, 1971) in analyses to avoid *a priori* character state transformations.

Additionally, a dataset of quantitative morphological characters was prepared that included 24 morphometric ratios, the measurement of total body length, and the dextral pectinal tooth count for the adult male and female, resulting in a total of 48 characters (Supplementary Table S4). Total body length was converted to a ratio (divided by 100) to avoid overweighting (Goloboff et al., 2006). These quantitative characters represent the range (e.g., minimum–maximum) and mean ratios and counts for each species, calculated from 49 measurements and seven meristic counts recorded in 74 specimens ($n = 39$ ♂, 35 ♀), as described by Cain et al. (2021): *B. amitaii* (5 ♂, 5 ♀); *B. arenicola* (2 ♂); *B. arava* (7 ♂, 1 ♀); *B. leptochelys* (1 ♂, 4 ♀); *B. levyi* (8 ♂, 9 ♀); *B. nitzani* (8 ♂, 10 ♀); *B. yotvatensis* (8 ♂, 6 ♀). Cain et al. (2021) also conducted non-metric multidimensional scaling (NMDS) and permutational multivariate analysis of variance (ADONIS) on the 24 ratios and counts for each sex.

2.5. Sequence alignment and statistics

Sequences were aligned using MAFFT v. 7.402 on the CIPRES Science Gateway (https://www.phylo.org; Miller et al., 2010). The COI and ITS2 loci were aligned using the G-INS-i alignment strategy, whereas the ribosomal 12S, 16S and 28S loci were aligned using the Q-INS-i strategy, which considers the secondary structure of RNA. Alignments were checked using Mesquite v. 3.5 (Maddison and Maddison, 2019). The alignment length of each locus was as follows: 12S: 281 bp; 16S: 270 bp; COI: 616 bp; 28S: 510 bp; ITS2: 541 bp (Table 2). The aligned loci were concatenated to create a multilocus molecular dataset with a total alignment length of 2218 bp. Mean nucleotide composition, number of variable positions and parsimony-informative sites, and percentage of transitions and transversions using a maximum composite likelihood method were calculated for each locus and the concatenated dataset in MEGA v. 10.1.7 (Tamura et al., 2004; Tamura et al., 2013; Kumar et al., 2018, Stecher et al., 2020). MEGA was also used to calculate mean uncorrected pairwise genetic distances, within and between species of *Buthacus*, for the COI locus.

2.6. Phylogenetic analysis

The molecular dataset (2218 aligned bp) and 22 qualitative morphological characters were concatenated and analyzed simultaneously using parsimony, Bayesian Inference (BI) and Maximum Likelihood (ML). Simultaneous analysis of molecular and morphological datasets, also known as the "total evidence" approach, increases explanatory power (see discussion and citations in Prendini et al., 2003)

and is particularly helpful when molecular data are missing for some taxa or when testing groups with relatively conservative morphology (Wilson et al., 2020), as in the present study. The molecular dataset and qualitative morphological characters were also concatenated with the 48 quantitative morphological characters (24 for each sex) and analyzed simultaneously using parsimony, however, for these analyses, the qualitative morphological dataset was reduced to seventeen characters by deactivating five characters (1, 3–5 and 12) which were not independent of some of the quantitative characters (Supplementary Tables S3, S4). The molecular dataset was also analyzed separately using parsimony, BI and ML.

Parsimony analyses were performed in TNT v. 1.1 (Goloboff et al., 2003, 2008). Gaps were treated as missing data, uninformative characters inactivated with the command *xinact*, and quantitative characters analyzed as such. The dataset was analyzed using equal weighting and implied weighting with five values of the concavity constant (k = 1, 3, 10, 60, 100). A script from Santibáñez-López et al. (2014), that was modified from Dimitrov et al. (2012, 2013) and includes tree drifting, tree fusing and mixed sectorial searches, was used to find the most parsimonious trees: *hold 10000; rseed1; xm: noverb nokeep; rat: it 0 up 4 down 4 au 0 num 36 give 99 equa; dri: it 10 fit 1.00 rfi 0.20 aut 0 num 36 give 99 xfa 3.00 equa;* sec*: mins 45 maxs 45 self 43 incr 75 minf 10 god 75 drift 6 glob 5 dglob 10 rou 3 xss 10–14 + 2 noxev noeq; tf: rou 5 minf 3 best ke nochoo swap; xm: level 10 nochk rep 50 fuse 3 dri 10 rss css noxss mult nodump conse 5 conf 75 nogive notarg upda autoc 3 xmix; xm; xmult*. Jackknife support was evaluated using a script from Dimitrov et al. (2012): *hold 10000; rseed1; mult: noratchet repl 10 tbr hold 1; resample jak repl 1000 freq from 0 [mult]*. A bootstrap analysis with 1000 replicates was performed for comparison.

Bayesian Inference was performed in MrBayes v. 3.2.7a (Ronquist and Huelsenbeck, 2003) on CIPRES. The dataset was partitioned by loci and parameters were unlinked across all partitions. Models for each molecular partition were selected using the Akaike Information Criterion in jModelTest v. 2.1.6 (Guindon and Gascuel, 2003; Darriba et al., 2012) on CIPRES. A gamma distribution, i.e., the Lewis (Mk) model (Lewis, 2001), was applied to the morphological partition. The analysis was run for 5 million generations or until the standard deviation of the split frequencies was 0.01, with the following settings: *mcmc; nchains = 4; print frequency = 1000; sample frequency = 1000; diagnosing frequency = 1000; burnin = 0.25; savebrlens = yes*. Nodal support was evaluated using posterior probabilities.

The ML analysis was performed in RAxML v. 8.2.12 (Stamatakis, 2006, 2014) on CIPRES. The dataset was partitioned by loci and a multigamma model applied to the five molecular partitions, whereas the Lewis (Mk) model (Lewis, 2001) was applied to the morphological partition. A rapid bootstrap analysis was used to search for the best scoring ML tree and nodal support evaluated with 1000 iterations of rapid bootstrapping. Individual loci were also analyzed separately in RAxML using a GTRGAMMA model.

2.7. Divergence time estimation analysis

A divergence time estimation analysis was performed on the molecular dataset using BEAST v. 1.10.4 (Drummond et al., 2012) on CIPRES. The dataset was trimmed to one terminal per species with ingroup exemplar terminals chosen based on geographical proximity to the type locality of each species, and rooted on *A. amoreuxi*. Sequences in the reduced molecular dataset were aligned using methods described above with xml files prepared in BEAUti v. 1.10.4 (Drummond et al., 2012). The dataset was partitioned by loci and site models were unlinked across all partitions. The site model for each partition was chosen using the Bayesian Information Criterion in jModelTest v. 2.1.6 (Guindon and Gascuel, 2003; Darriba et al., 2012). Tree models were linked across all partitions and a Birth–Death model applied. Clock models were unlinked across all partitions and an uncorrelated lognormal molecular clock chosen for each partition. As no closely related fossil taxa were available, the analysis was calibrated using published molecular clock rates for scorpions (Gantenbein and Largiadèr, 2002; Gantenbein et al., 2005; Graham et al., 2012, 2013a,b, 2017, 2019; Bryson et al., 2013a,b, 2014). The ucld.mean was set to a normal distribution for the COI and 16S loci with the following settings: $\mu = 0.007$, $\sigma = 0.00146$ for COI and $\mu = 0.005$, $\sigma = 0.00270$ for 16S (Graham et al., 2019). A uniform prior was applied to the ucld.mean for the 12S, 28S and ITS2 loci, with the following settings: min = 0.002, max = 0.5 for 12S, and min = 0.0001, max = 0.01 for 28S and ITS2 (Bryson et al., 2013a). A Markov Chain Monte Carlo (MCMC) analysis with 500 million generations, sampling every ten thousand generations, was performed in two independent searches. Tracer v. 1.7.1 (Rambaut et al., 2014) was used to ensure that Effective Sample Size (ESS) values were >200 and assess convergence of the two independent runs. Tree files were combined in LogCombiner v. 1.10.4, removing the first 25% of samples as burnin. TreeAnnotator v. 1.10.4 was used to find the maximum clade credibility tree of the combined tree files.

2.8. Ancestral range estimation

An ancestral range estimation analysis was performed on the time-calibrated phylogeny using the R package BioGeoBEARS v. 1.1.1 (Matzke, 2013a,b, 2014). The *drop.tip* function from the R package ape (Paradis et al., 2004) was used to remove the outgroup, *A. amoreuxi*, and the *force.ultrametric* function from the R package phytools (Revell, 2012), to constrain the tree to be ultrametric. Four biogeographical areas were defined following Machado et al. (2020): west of the Nile River; east of the Nile River; the Levant; and the Arabian Peninsula. Terminal species were scored as present or absent in each area. The maximum number of areas that a given species was allowed to occupy was set to four. Three models, Dispersal-Extinction-Cladogenesis (DEC), DIVALIKE, and BAYAREALIKE, were tested, and an additional jump dispersal parameter (j) tested for each model. Statistical analyses produced log-likelihoods of each model and the best model was selected using the corrected Akaike Information Criterion (AICc), appropriate for small datasets (Supplementary Table S5).

3. Results

3.1. DNA sequence composition and pairwise distances

As in other scorpion families (Prendini et al., 2003; González-Santillán and Prendini, 2015), the mitochondrial loci were more variable. The proportion of variable and parsimony-informative sites in the mitochondrial 12S, 16S and COI loci was 34%, 33%, 26% and 26%, 27%, 21%, respectively (Table 2). In contrast, only 3% of the sites were variable and 2% parsimony-informative in the nuclear 28S. These low values are similar to those reported in a species-level analysis of scorpions (Talal et al., 2015) and predictably lower than reported in genus-level analyses (Prendini et al., 2003; González-Santillán and Prendini, 2015). Nevertheless, as shown in scorpions and other arthropods (e.g., Wiemers et al., 2009; Bryson et al., 2013a), the nuclear ITS2 fragment contained more variable (29%) and parsimony-informative (15%) sites. A total of 518 (23%) sites were variable and 365 (16%) parsimony-informative in the concatenated dataset. The estimated overall transition to transversion ratio (ts:tv; Table 2) was 0.71, higher than the expected value of 2 (González-Santillán and Prendini, 2015). The mitochondrial loci were characterized by an AT-bias, with 73% mean AT-content for 16S and 12S, and 62% mean AT-content for COI, whereas the nuclear loci were more GC-rich with 57% and 53% mean GC-content for 28S and ITS2, respectively (Table 2).

Mean uncorrected pairwise distances of the COI locus varied from 11.6 to 13.7% between *A. amoreuxi* and the seven species of *Buthacus* (Table 3). Among the species of *Buthacus*, mean uncorrected pairwise distances of the COI locus were highest between *B. levyi* and *B. nitzani* (11.2%) and lowest between *B. leptochelys* and *B. nitzani* (2.1%). Mean

Table 3
Mean between-species and within-species (boldface) uncorrected pairwise (*p*) distances of the Cytochrome *c* Oxidase Subunit I locus for sand scorpions, genus *Buthacus* Birula, 1908 (Buthidae C.L. Koch, 1837): *Buthacus amitaii* Cain et al., 2021; *Buthacus arava* Cain et al., 2021; *Buthacus arenicola* (Simon, 1885); *Buthacus leptochelys* (Ehrenberg, 1828); *Buthacus levyi* Cain et al., 2021; *Buthacus nitzani* Levy et al., 1973; *Buthacus yotvatensis* Levy et al., 1973.

	B. amitaii	*B. arava*	*B. arenicola*	*B. leptochelys*	*B. levyi*	*B. nitzani*	*B. yotvatensis*
B. amitaii	**0.0024**						
B. arava	0.0993	**0.0027**					
B. arenicola	0.1032	0.0856	**0.0119**				
B. leptochelys	0.0360	0.1072	0.1063	**0.0082**			
B. levyi	0.1106	0.0870	0.0601	0.1088	**0.0067**		
B. nitzani	0.0296	0.1097	0.1074	0.0213	0.1116	**0.0137**	
B. yotvatensis	0.0990	0.0924	0.1007	0.1034	0.1076	0.1017	**0.0034**

uncorrected pairwise distances of the COI locus within species of *Buthacus* (Table 3) were lowest among populations of *B. amitaii* (0.2%) and highest among populations of *B. nitzani* (1.4%).

3.2. Phylogenetic analyses

Simultaneous analysis of the molecular dataset and 22 qualitative morphological characters with parsimony and equal weighting or implied weighting (k = 1, 3, 10, 60, or 100) recovered each species of *Buthacus* as monophyletic (Table 4). Relationships among the species were mostly consistent among the analyses except for the position of *B. nitzani*, placed sister to *B. leptochelys* in the parsimony analyses with equal weighting or implied weighting with k = 3, 10, or 100, but sister to *B. amitaii* in the analyses with implied weighting and k = 1 or 60. Simultaneous analysis of the molecular dataset and qualitative morphological characters with ML also recovered each species as monophyletic with high (≥93% for *B. arava*, *B. arenicola*, *B. levyi*, and *B. yotvatensis*) or moderate (64–76% for *B. leptochelys* and *B. nitzani*) bootstrap support, and placed *B. nitzani* sister to *B. amitaii* with moderate bootstrap support (69%). Simultaneous analysis of the molecular dataset and qualitative morphological characters with BI and ML, including ascertainment bias with Lewis correction, recovered each species as monophyletic with high posterior probabilities (≥0.92), except for *B. nitzani*, which was rendered paraphyletic by *B. leptochelys*. Relationships among the other species recovered with BI and ML with Lewis correction were identical to the relationships recovered with parsimony and ML, and received high support (≥0.93).

Simultaneous analysis of the molecular dataset, 48 quantitative morphological characters (analyzed as range and mean ratios), and 17 qualitative morphological characters with parsimony and equal weighting or implied weighting (k = 1, 3, 10, 60, or 100) recovered each species of *Buthacus* as monophyletic. Relationships among the species

Table 4
Nodal stability for species and clades in phylogenetic analysis of sand scorpions, genus *Buthacus* Birula, 1908 (Buthidae C.L. Koch, 1837), based on separate and simultaneous analysis of 22 (Qual) or 17 (Qual-r) qualitative morphological characters, 48 quantitative (Quan) morphological characters and 2218 aligned base-pairs of DNA from two nuclear and three mitochondrial loci (Mol) datasets using Maximum Likelihood (ML) including ascertainment bias with Lewis correction (ML-Asc), Bayesian Inference (BI) and parsimony with equal weighting (EW) or implied weighting (IW) with five values of the concavity constant (k). Black cells indicated clades and taxa recovered under various parameters. Species abbreviated as follows: *ami*: *Buthacus amitaii* Cain et al., 2021; *ara*: *Buthacus arava* Cain et al., 2021; *are*: *Buthacus arenicola* (Simon, 1885); *lep*: *Buthacus leptochelys* (Ehrenberg, 1828); *lev*: *Buthacus levyi* Cain et al., 2021; *nit*: *Buthacus nitzani* Levy et al., 1973; *yot*: *Buthacus yotvatensis* Levy et al., 1973.

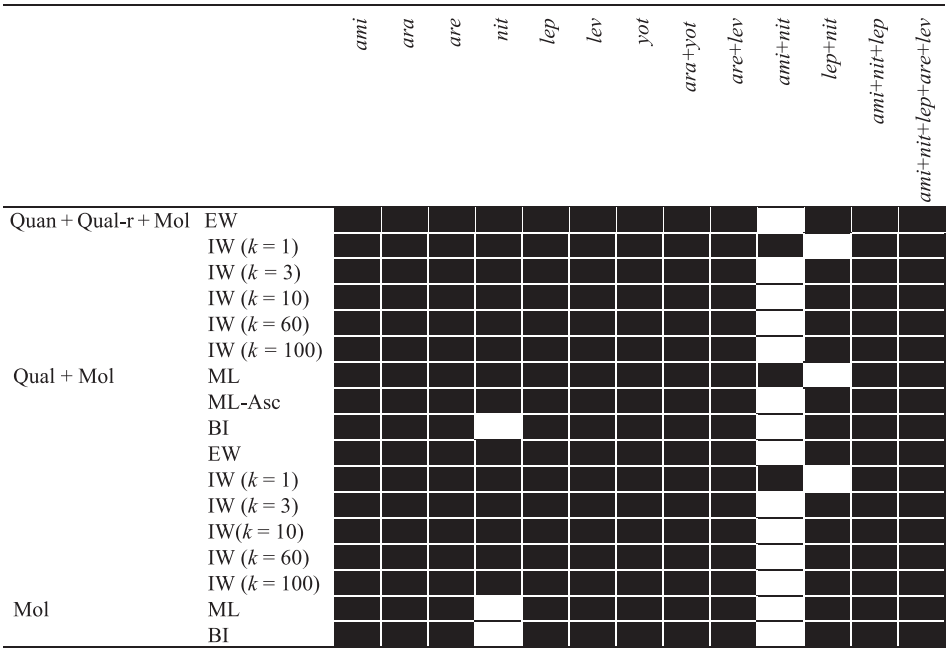

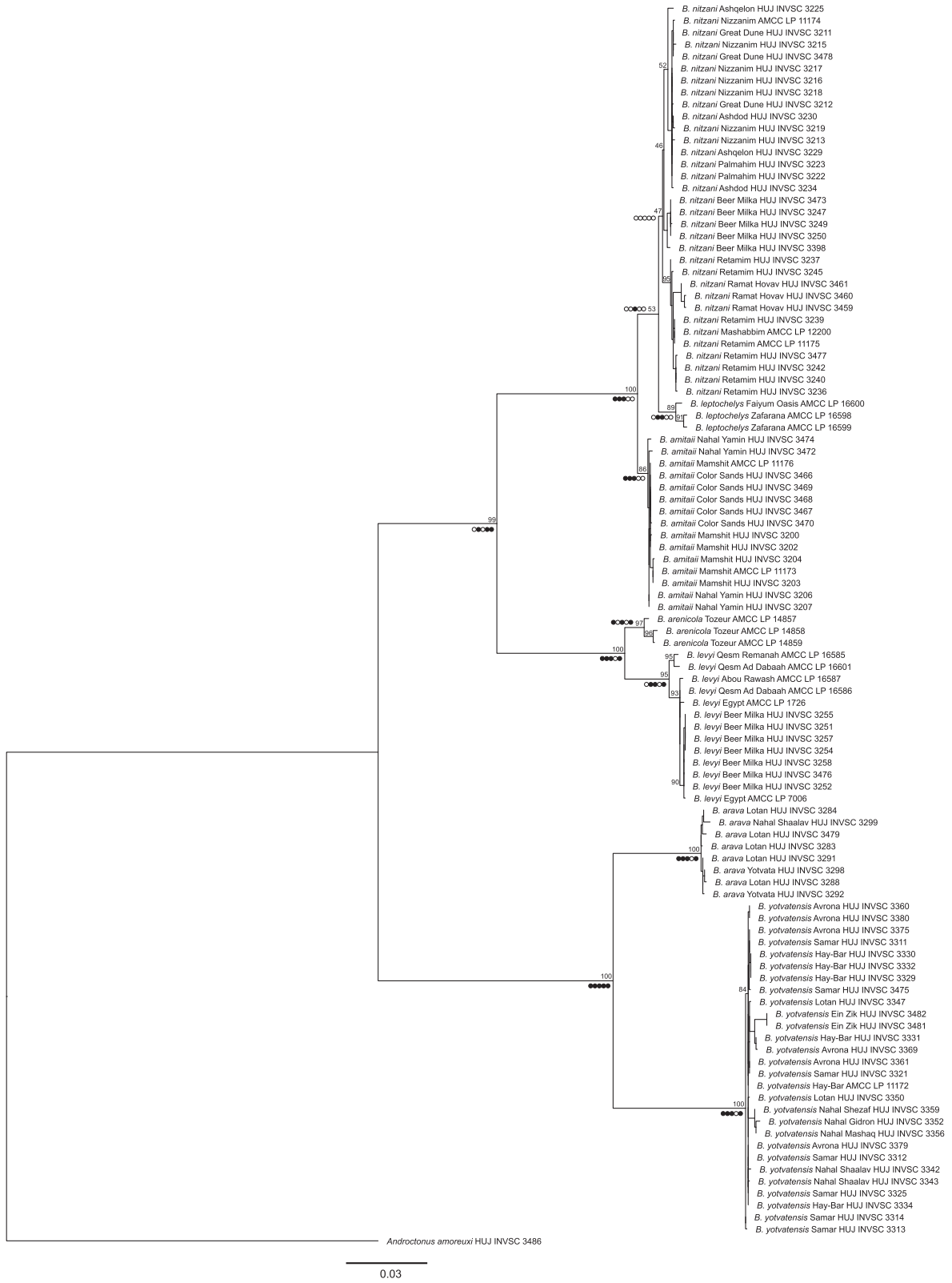

Fig. 3. Phylogeny of 104 samples of sand scorpions, genus *Buthacus* Birula, 1908 (Buthidae C.L. Koch, 1837) and an outgroup, *Androctonus amoreuxi* (Linneaus, 1758) inferred from Maximum Likelihood analysis of 22 qualitative morphological characters and 2218 aligned base-pairs of DNA sequence from three mitochondrial gene loci, 12*S* rDNA, 16*S* rDNA, and Cytochrome *c* Oxidase Subunit I, and two nuclear gene loci, 28*S* rDNA and the Internal Transcribed Spacer (ITS2). Lewis (Mk) model applied to morphological partition and GTRGAMMA model to molecular partition. Codes for terminals denote species, site and sample number (Supplementary Material S2). Bootstrap support values indicated at nodes. Nodal stability for species and clades in RAxML analysis of each locus represented by circles below nodes. Loci order (left to right): 12S, 16S, CO1, 28S, ITS. Black and white circles indicate supported and unsupported clades, respectively.

were consistent with simultaneous analyses of the molecular dataset and qualitative morphological characters except that *B. nitzani* was placed sister to *B. amitaii* in the analyses with equal weighting or implied weighting and $k = 1$, 60, or 100, and sister to *B. leptochelys* in the analyses with implied weighting and $k = 3$ or 10 (Table 4). Relationships among the species were congruent when quantitative characters were analyzed as range or mean ratios, however.

Separate analysis of the molecular dataset with ML or BI recovered each species as monophyletic except for *B. nitzani*, again rendered paraphyletic by *B. leptochelys* (Table 4). Each species and clade received high bootstrap (≥83%) and posterior probability (≥0.92) support values except the clade comprising *B. leptochelys* and *B. nitzani*, which received moderate bootstrap support (56%).

Despite the abovementioned differences, all analyses identified two major clades that were geographically-delimited (Fig. 3): an African clade comprising species distributed across North Africa, from Tunisia to the Sinai Peninsula, and into Israel, west of the Jordan Valley (i.e., *B. amitaii*, *B. arenicola*, *B. leptochelys*, *B. levyi* and *B. nitzani*), and an Asian clade comprising species from Israel and Jordan, in the southern part of the Jordan Valley (known as the Arava Valley), and to the east thereof (i.e., *B. arava* and *B. yotvatensis*).

The African clade was further divided into two subclades. One subclade comprised *B. leptochelys* from Egypt (sites 10–12 in Table 1; Fig. 2B), and *B. amitaii* and *B. nitzani* from the Negev Desert in Israel (sites 1–9 and 13–15 in Fig. 2C). The other subclade comprised *B. arenicola* from Tunisia (sites 16–18 in Fig. 2A) and *B. levyi* from Israel, Sinai and mainland Egypt (sites 9 and 20–23 in Fig. 2B, C), and two additional specimens from mainland Egypt without accurate locality data (site 19 in Table 1). Specimens collected in close proximity (sites 9 and 20) to localities from which *B. arenicola* was previously reported in Sinai (Levy and Amitai, 1980) were found to be distinct from populations in the vicinity of the type locality of *B. arenicola* in Tunisia (Table 1, Figs. 2, 3), and grouped together with specimens from mainland Egypt, including localities west of the Nile River (Fig. 2B), justifying their recognition as a distinct species, *B. levyi*, by Cain et al. (2021).

The Asian clade comprised specimens of *B. arava* and *B. yotvatensis* (Fig. 3) from localities in the Arava Valley (sites 24–29 and 31–33 in Fig. 2C), extending slightly west to Ein-Zik (site 30 in Fig. 2C).

3.3. Divergence time estimation analysis

The divergence time estimation analysis produced a fully dichotomous tree (Fig. 4), congruent with results of the phylogenetic analyses described above: (*A. amoreuxi* ((*B. arava B. yotvatensis*) ((*B. arenicola B. levyi*) (*B. amitaii* (*B. leptochelys B. nitzani*))))). The monophyly of species and clades received high posterior probability support (≥0.89). Divergence between the ancestors of the African and Asian clades occurred around 19 Ma whereas divergence between the ancestors of *B. arava* and

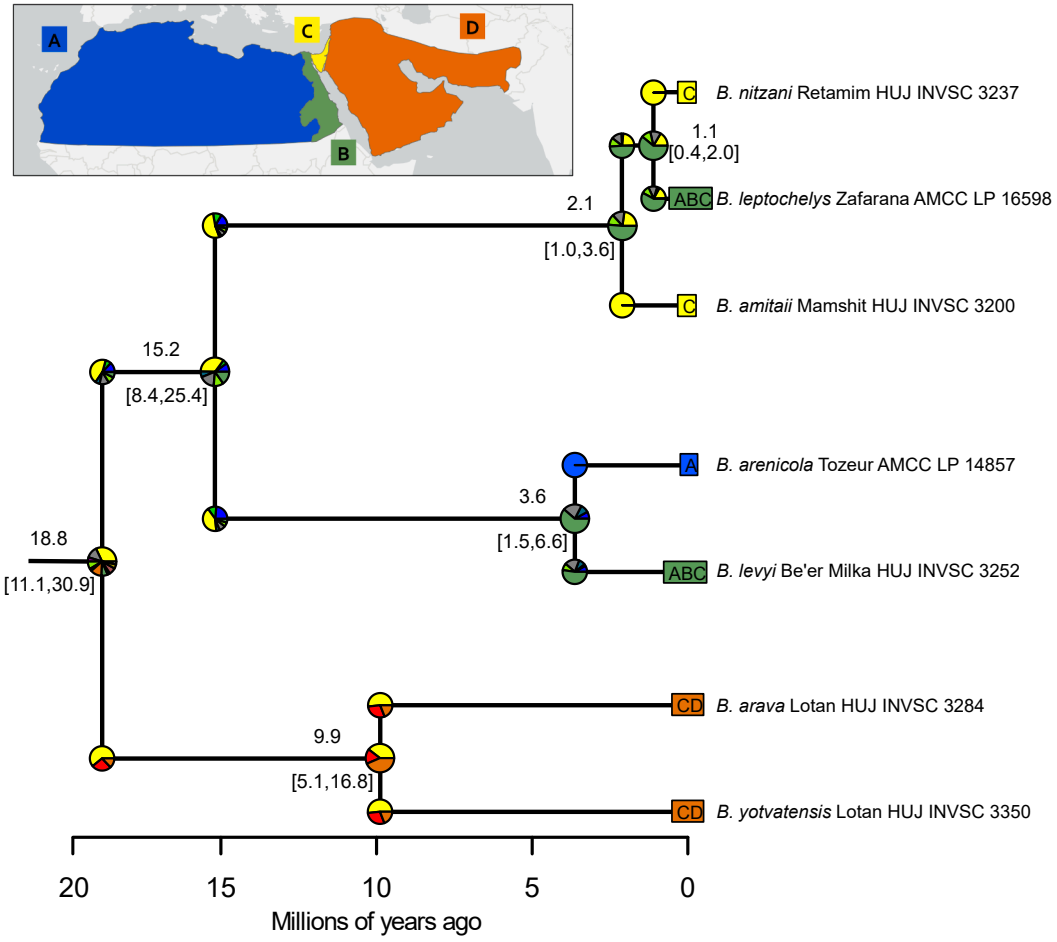

Fig. 4. Estimation of ancestral ranges of sand scorpions, genus *Buthacus* Birula, 1908 (Buthidae C.L. Koch, 1837) across four biogeographical areas, using BioGeoBEARS: (**A**) west of the Nile River; (**B**) east of the Nile River; (**C**) the Levant; (**D**) the Arabian Plate. Reconstructions plotted on dated phylogeny produced using BEAST v. 1.10.4 after analysis of 2202 aligned base-pairs of DNA sequence from three mitochondrial gene loci, 12S rDNA, 16S rDNA, and Cytochrome *c* Oxidase Subunit I, and two nuclear gene loci, 28S rDNA and the Internal Transcribed Spacer 2 (ITS2), for reduced dataset comprising one exemplar terminal per species and an outgroup, *Androctonus amoreuxi* (Linneaus, 1758). Numbers at nodes indicate divergence dates in millions of years (Ma). Regions-map constructed with ArcGIS Pro v. 2.6.0. Median ages presented above nodes and 95% confidence interval of median ages presented below.

B. yotvatensis occurred around 10 Ma, and between the two subclades of the African clade (i.e., the subclade comprising *B. arenicola* and *B. levyi*, and the subclade comprising *B. amitaii*, *B. leptochelys*, and *B. nitzani*), around 15 Ma.

3.4. Ancestral range estimation

The DEC model was chosen as the most appropriate due to the lowest log likelihood and best AICc score (Supplementary Table S5). The following ancestral ranges were recovered for each species based on this model: Arabian Peninsula for *B. arava* and *B. yotvatensis*; the Levant for *B. amitaii* and *B. nitzani*; and west of the Nile River for *B. arenicola*. The ancestral ranges for *B. leptochelys* and *B. levyi* encompassed North Africa (east and west of the Nile River) and the Levant. The Levant was recovered as the ancestral area for the African clade and the Arabian Peninsula as the ancestral area for the Asian clade.

4. Discussion

4.1. African and Asian clades separated by Great Rift Valley

The analyses presented here identified two distinct clades: an African clade, represented within the study area by species extending from Tunisia (*B. arenicola*), through Egypt and Sinai (*B. leptochelys*, *B. levyi*), the western Negev Desert and southern coastal plain of Israel (*B. nitzani*), to the northern Negev Desert (*B. amitaii*), and an Asian clade, represented by species inhabiting the southern part of the Jordan Valley (i.e., the Arava Valley) and vicinity (*B. arava* and *B. yotvatensis*) (Fig. 2). The recognition of two geographically-delimited clades of *Buthacus* in Africa and Asia, approximately separated by the Jordan Valley (the Jordan Rift Valley or Syro-African Depression), the northernmost part of the Great Rift Valley, which extends all the way to southern Africa, was also supported by morphological evidence, including an NMDS analysis in which *B. arava* and *B. yotvatensis* clustered separately from five *Buthacus*

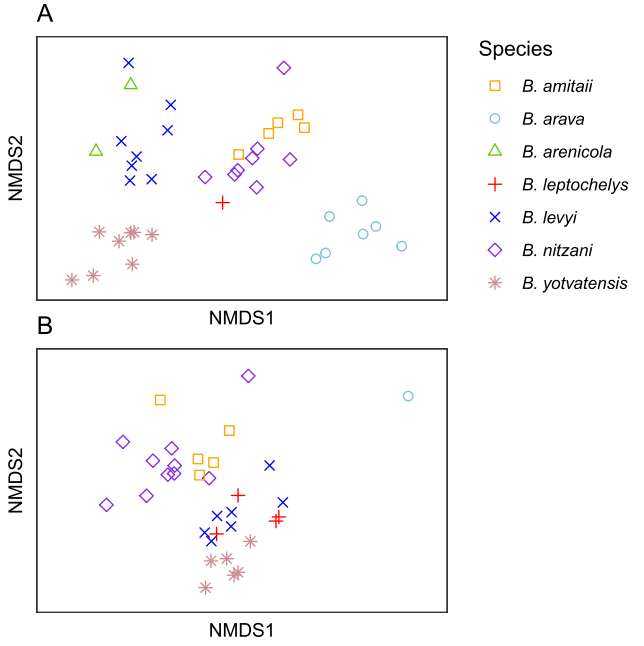

Fig. 5. Nonmetric multidimensional scaling (NMDS) plots of adult males (**A**) and females (**B**) of sand scorpions, genus *Buthacus* Birula, 1908 (Buthidae C.L. Koch, 1837), reproduced from Cain et al. (2021): *Buthacus amitaii* Cain et al., 2021; *Buthacus arava* Cain et al., 2021; *Buthacus arenicola* (Simon, 1885); *Buthacus leptochelys* (Ehrenberg, 1828); *Buthacus levyi* Cain et al., 2021; *Buthacus nitzani* Levy et al., 1973; *Buthacus yotvatensis* Levy et al., 1973.

species occurring west of the Jordan Valley (Cain et al., 2021; Fig. 5).

These findings were independently recovered in a recent phylogenetic analysis by Alqahtani and Badry (2020), based on 16S rDNA sequences for seven ingroup terminals, representing three species of *Buthacus*, which recovered a clade comprising two African species, *B. arenicola* and *B. leptochelys*, to the exclusion of an Asian species, *B. nigroaculeatus*. Whereas the Egyptian samples referred to as *B. arenicola* by Alqahtani and Badry (2020) are undoubtedly conspecific with *B. levyi*, as defined by Cain et al. (2021), *B. nigroaculeatus* is closely related to *B. yotvatensis*, and was originally described as a subspecies thereof (Levy et al., 1973). As such, the findings of Alqahtani and Badry (2020) are directly comparable with the study presented here, which was based on a far more extensive dataset and more exhaustive analyses.

Numerous morphological characters differentiate members of the African and Asian clades of *Buthacus*. For example, the total body length of species in the Asian clade is often greater than that of species in the African clade (Table 5), and the tegument surfaces (notably the carapace, pedipalps, mesosomal tergites, metasoma and telson) are typically more granular in species of the Asian clade than species of the African clade, in which the surfaces are more glabrous. Morphological differences characterizing the two clades are shared by other species not included in the phylogenetic or NMDS analyses. For example, *B. arava* and *B. yotvatensis* share characters such as the granular tegument surfaces with other *Buthacus* species occurring east of the Jordan Valley, such as *B. nigroaculeatus*, from the Arabian Peninsula, and *Buthacus tadmorensis* (Simon, 1892), which extends across the Fertile Crescent, from northern Jordan, Syria, and Turkey, to Iraq and Iran (Cain et al., 2021).

Although it is conceivable that the African and Asian clades may constitute different genera, a notion first suggested for *B. yotvatensis* by Levy et al. (1973), implementing such a move would be premature, as the matter requires a more extensive phylogenetic analysis, including a broader sample of taxa. As noted by Cain et al. (2021), the limits of *Buthacus* with respect to several other psammophilous Palearctic buthid genera, e.g., *Buthiscus* Birula, 1905, *Gint* Kovařík et al., 2013, *Liobuthus* Birula, 1898, *Pectinibuthus* Fet, 1984, *Plesiobuthus* Pocock, 1900, *Trypanothacus* Lowe et al., 2019, and *Vachoniolus* Levy et al., 1973, some of which include species previously assigned to *Buthacus* (Kovařík et al., 2013, 2016; Kovařík, 2018; Lowe et al., 2019; Alqahtani and Badry, 2020), remain unclear. Kovařík et al. (2016) suggested, without presenting phylogenetic evidence, that *Buthacus* might be paraphyletic because many of the putative diagnostic characters for the genus appear to be plesiomorphic. A rigorous test of the monophyly of *Buthacus*,

Table 5
Total body length (mm) for adult male and female sand scorpions, genus *Buthacus* Birula, 1908 (Buthidae C.L. Koch, 1837): *Buthacus amitaii* Cain et al., 2021; *Buthacus arava* Cain et al., 2021; *Buthacus arenicola* (Simon, 1885); *Buthacus leptochelys* (Ehrenberg, 1828); *Buthacus levyi* Cain et al., 2021; *Buthacus nitzani* Levy et al., 1973; *Buthacus yotvatensis* Levy et al., 1973.

Clade	Species	Sex	*n*	min	max
African	*B. amitaii*	♂	5	48.02	58.87
		♀	5	48.49	50.78
	B. arenicola	♂	2	54.26	54.39
	B. leptochelys	♂	1	63.71	63.71
		♀	4	63.15	68.00
	B. levyi	♂	8	45.44	52.57
		♀	9	53.61	62.03
	B. nitzani	♂	8	47.46	58.53
		♀	10	44.38	54.57
Asian	*B. arava*	♂	7	61.77	75.00
		♀	1	62.29	62.29
	B. yotvatensis	♂	8	61.88	71.88
		♀	6	71.66	85.06

which was beyond the scope of the present study, is in preparation.

4.2. Invalid species groups

The African and Asian clades invalidate the traditionally recognized *B. arenicola* and *B. leptochelys* groups, based primarily on the count of retrolateral accessory denticles on the movable finger of the pedipalp chela and, to a lesser extent, the pilosity of the metasoma (Levy et al., 1973; Levy and Amitai, 1980; Kovařík, 2005; Alqahtani and Badry, 2020). As originally proposed, species of the *B. leptochelys* group bear a complete, or almost complete, series of retrolateral accessory denticles on the chela movable finger, compared with species of the *B. arenicola* group, in which all or most of the retrolateral accessory denticles are absent (Levy et al., 1973; Levy and Amitai, 1980). Although Lourenço (2006) questioned the diagnostic value of retrolateral accessory denticles on the movable finger in *Buthacus*, based on significant variation observed within the *B. arenicola* and *B. leptochelys* groups, the character remained in widespread use (Kovařík, 2005; Lourenço, 2006; Zambre and Lourenço, 2010; Lourenço and Sadine, 2015; Kovařík et al., 2016; Kovařík, 2018; Alqahtani and Badry, 2020).

Cain et al. (2021) confirmed the doubts of Lourenço (2006) concerning the utility of retrolateral accessory denticles on the movable finger in *Buthacus*. Some species of *Buthacus* were more likely to possess a complete series of denticles whereas others lacked them altogether, and an overlap was observed in the number of denticles between *B. amitaii* (0–10, $n = 10$) and *B. levyi* (0–5, $n = 16$), representing the *B. leptochelys* and *B. arenicola* groups, respectively. The phylogenetic analyses presented here further reinforce the conclusion that the two species groups constitute a false dichotomy. *Buthacus leptochelys* and *B. nitzani*, previously assigned to the *B. leptochelys* group (Levy et al., 1973; Levy and Amitai, 1980), were monophyletic with *B. arenicola*, of the *B. arenicola* group, to the exclusion of *B. yotvatensis*, also previously assigned to the *B. leptochelys* group, rendering the *B. leptochelys* group paraphyletic (Fig. 3).

As with counts of retrolateral accessory denticles on the chela movable finger, metasomal pilosity cannot be used to separate the two groups (contra Levy et al., 1973; Alqahtani and Badry, 2020). Although densely setose in several species of the Asian clade, e.g., *B. nigroaculeatus*, *B. tadmorensis* and *B. yotvatensis*, the metasoma and telson are sparsely setose in the closely related *B. arava*, as in species of the African clade previously assigned to the *B. arenicola* and *B. leptochelys* groups (Cain et al., 2021).

4.3. Species limits and cryptic diversity

The limits of two African species, *B. arenicola* and *B. leptochelys*, resolved by the morphological investigation of Cain et al. (2021), were confirmed by the phylogenetic analyses presented here. Levy and Amitai (1980) noted that the distributions of *B. arenicola* and *B. leptochelys* overlap in parts of Egypt and that the population of *B. arenicola* in the Sinai Peninsula differs morphologically from the population in Algeria and Tunisia, suggesting it may represent a distinct subspecies, an opinion shared by Lourenço (2006). Following examination of the types of *B. arenicola* and *B. leptochelys*, in addition to material from the vicinity of the type locality of *B. arenicola*, in Tunisia, and from mainland Egypt, the Sinai Peninsula, and Israel, Cain et al. (2021) confirmed the distinction between *B. arenicola* and *B. leptochelys*, and previous suggestions that the population of *B. arenicola* in Egypt and Israel is distinct from the typical population in Algeria and Tunisia (Levy and Amitai, 1980; Lourenço, 2006). The phylogenetic analyses presented here, which include specimens from the vicinity of the type locality of *B. arenicola* in Tunisia, and from mainland Egypt and the Sinai Peninsula, confirmed that *B. arenicola* is restricted to central Tunisia and northeastern Algeria, and the population previously identified as *B. arenicola* from Egypt and Israel represents a distinct species, described by Cain et al. (2021) as *B. levyi*. The two allopatric species (Fig. 2) form well-supported clades (Fig. 3), and differ morphologically (ADONIS: $R^2 = 0.36$, $Pr = 0.043$; Fig. 5).

The analyses presented here also supported the elevation of *B. nitzani*, originally described as a subspecies of *B. leptochelys* (Levy et al., 1973; Levy and Amitai, 1980), to the rank of species by Cain et al. (2021). Although not reciprocally monophyletic in the separate analyses of the molecular dataset or the simultaneous analysis of the morphological and molecular datasets with BI, *B. leptochelys* and *B. nitzani* were reciprocally monophyletic in all other simultaneous analyses. This finding, taken together with their consistent morphological differences, confirmed by the NMDS analysis (Fig. 5), justifies their recognition as distinct species. *Buthacus leptochelys* is restricted to mainland Egypt and the Sinai Peninsula, whereas *B. nitzani* is endemic to Israel (Cain et al., 2021).

The phylogenetic analyses presented here also revealed a cryptic species, described by Cain et al. (2021) as *B. amitaii*. Specimens from three sites in the northeastern Negev Desert (sites 13–15 in Fig. 2C), including material identified as *B. leptochelys* by Levy and Amitai (1980), were consistently separated from *B. leptochelys* and *B. nitzani* by all phylogenetic analyses, despite failing to separate clearly in the NMDS analysis (Fig. 5). Upon closer examination, distinct morphological characters were observed in these specimens, e.g., the posterior granules on the ventrosubmedian and ventrolateral carinae of the second and third metasomal segments, and the ventrolateral carinae of the fifth segment, were much more pronounced than in *B. nitzani* (Cain et al., 2021). Such processes are considered an ecomorphological adaptation in species which use the metasoma for loosening hard, gritty soil in burrow construction (Barahoei et al., 2021; Prendini, 2001a,b; Prendini et al., 2003), consistent with the compacted sand and loess typical of the northeastern Negev Desert, inhabited by *B. amitaii* (Singer, 2007). In contrast, the smooth ventral surfaces of the metasomal segments of *B. nitzani* are consistent with the semi-consolidated to unconsolidated sand dunes in which this species occurs (sites 1–9 in Fig. 2C).

Despite the superficial similarity between *B. arava* and *B. nitzani*, both of which inhabit semi-consolidated to unconsolidated sand dunes, the phylogenetic analyses (Fig. 3) confirmed the NMDS analysis (Fig. 5) that this similarity is convergent. *Buthacus arava* is a member of the Asian clade, more closely related to the morphologically disparate *B. yotvatensis*, with which it is sympatric at several localities (e.g., sites 24–26 in Fig. 2C). The many morphological differences between *B. arava* and other species in the Levant are elaborated by Cain et al. (2021).

4.4. The Levant as crossroads between Africa and Asia

Most of the Negev Desert and Sinai Peninsula form part of the phytogeographical Saharo-Arabian region, with sandy desert habitats extending along the coastal plain of Israel to the southern part of the Jordan Valley, known as the Arava Valley (Kugler, 1988), and neighboring countries in Asia. The colonization of this area by Saharan elements is attributed to dispersal along the narrow stretch of sand dunes in northern Sinai and the southern coastal plain by psammophilous taxa (Tchernov, 1988). These African and Asian influences match the two major clades reported here. The location of the Levant as a continental crossroads, combining Asian and African influences, is further exemplified by the distribution of other psammophilous taxa. For example, among horned vipers (*Cerastes* Laurenti, 1768) and short-fingered geckos (*Stenodactylus* Fitzinger, 1826), the Arava Valley represents the westernmost tip of the Asian species, *Cerastes gasperettii* Leviton and Anderson, 1967, and *Stenodactylus doriae* (Blandford, 1874), whereas *Cerastes vipera* (L., 1758) and *Stenodactylus petrii* J. Anderson, 1896 from North Africa and Sinai, extend northeast to the western Negev (Werner, 1988; Werner et al., 1991; Fujita and Papenfuss, 2011; IUCN 2019). Similarly, in mammals, the psammophilous gerbil, *Gerbillus nanus* Blanford, 1875, is distributed in Asia, the Arabian Peninsula, and the Arava Valley, whereas the North African gerbils, *Gerbillus andersoni* de Winton, 1902 and *Gerbillus pyramidum* Geoffroy, 1825, extend along the

coastal plain of Israel, but do not reach the Arava Valley (Abramsky et al., 1985).

The patterns of distribution of African and Asian taxa in Israel and the Sinai Peninsula are best explained by plate tectonics. Approximately 20 Ma, the Afro-Arabian plate collided with the Eurasian plate, connecting the two continents via the Gomphotherium Landbridge (Rögl, 1999; Harzhauser et al., 2007; Hou and Li, 2018; Georgalis et al., 2020), which existed in present-day Turkey, Syria and Iraq. Several studies hypothesized that the formation of this land bridge was crucial for faunal exchange between Africa and Asia, enabling many vertebrate taxa to move across in both directions (Pook et al., 2009; Sen, 2013; Kapli et al., 2015; Machado et al., 2020). Further south, the Levantine Corridor, spanning the Jordan Valley between Israel and Jordan, provided another land bridge for dispersal between Africa and Asia from the Early Miocene onwards (López-Antoñanzas et al., 2016, 2019; Grossman et al., 2019). The divergence time estimation analysis of sand scorpions presented here supports these hypotheses, as the African and Asian clades of *Buthacus* diverged in the Early Miocene (19 Ma) and the Levant was the ancestral area for both clades (Fig. 4). More recent divergences reported here between *B. amitaii*, from the northeastern Negev Desert, and *B nitzani* from the western Negev Desert and southern coastal plain of Israel, may be have resulted from uplift of the Central Negev within the last 2 Ma (Horowitz, 1988).

5. Conclusions

The study presented here set out to resolve the systematics and biogeography of the sand scorpions, genus *Buthacus*, occurring in the Levant. The results invalidate the traditional *B. arenicola* and *B. leptochelys* species groups. Instead, two geographically-delimited clades were recovered, representing African and Asian lineages, the divergence of which coincides temporally with the existence of land bridges that facilitated dispersal between Africa and Asia in the Early Miocene. The results agree with a previous study of *Buthacus* based on a single mitochondrial locus, and with biogeographical studies of other taxa in the region. Although the sampling includes only a small proportion of the known species of *Buthacus* and focuses on the Levant, the results provide a starting point for understanding the origins and diversification of this widespread Palearctic scorpion genus. The inclusion of additional species from across the distribution in future investigations will clarify the systematic limits and biogeographical history of sand scorpions in more detail.

CRediT authorship contribution statement

Shlomo Cain: Validation, Formal analysis, Investigation, Resources, Data curation, Writing - original draft, Writing - review & editing, Visualization. **Stephanie F. Loria:** Formal analysis, Writing - original draft, Writing - review & editing. **Rachel Ben-Shlomo:** Methodology, Formal analysis, Resources, Supervision. **Lorenzo Prendini:** Conceptualization, Formal analysis, Investigation, Resources, Data curation, Writing - review & editing, Supervision, Project administration, Funding acquisition. **Eran Gefen:** Conceptualization, Investigation, Resources, Writing - original draft, Writing - review & editing, Supervision, Project administration, Funding acquisition.

Declaration of Competing Interest

The authors declare that they have no known competing financial interests or personal relationships that could have appeared to influence the work reported in this paper.

Acknowledgments

This research was funded by U.S.-Israel Binational Science Foundation award (BSF #2014046) to L.P. and E.G. The 26th European Congress of Arachnology and Ben-Gurion University of the Negev (BGU), Israel, partially supported L.P.'s visit to Israel in 2011, and the Israel Taxonomy Initiative and BGU (Jacob Blaustein Center for Scientific Cooperation) supported his visit in 2013. We thank Efrat Gavish-Regev (HUJ), Sergei Zonstein and Ariel-Leib-Leonid Friedman (SMNH), and Christoph Hörweg (NHMW) for lending type and nontype material from collections in their care; Jason Dunlop (ZMB), and Elise-Anne Leguin (MNHN) for images of type material; Rotem Agmon, Ayelet Allon, Nadav Amir, Zuhair Amr, Essam Attia, Jamel Babay, Tharina Bird, Noach Braun, Efrat Gavish-Regev, Gal Geisler, Fenik S. Hussen, Colleen Irby, Manel Khammasi, David Kotter, Reut Less, Snir Livne, Yael Lubin, Mor Lugassi, Asia Novikova, Itamar Ofer, Yael Olek, Ridha Ouina, Avner Rinot, Nitzan Segev, Boaz Shacham, Stav Talal, Itay Tesler, and Yoram Zvik, for donating material and/or assisting the authors with fieldwork; the Israel Nature and National Parks Protection Authority for permission to collect and export scorpions from Israel (permits 2011/38157 and 2013/39974 to L.P. 2015/41081, 2017/41728 to E.G., and 2017/41779 to Efrat Gavish-Regev); Essam Attia and Hisham K. El-Hennawy for hospitality, logistics and permissions in Egypt; Zuhair Amr and the Royal Jordanian Society for the Conservation of Nature for hospitality, logistics and permissions in Jordan; Saïd Nouira, Jamel Babay and Ridha Ouina for hospitality and logistics in Tunisia; Diogo Casellato, Deborah Chin, Ofelia Delgado-Hernandez and Tarang Sharma for generating DNA sequence data at the AMNH; Andrew Fatiukha, Stav Talal and Tamar Krugman for assistance with generating sequence data at the Institute of Evolution, University of Haifa; Emile Cain and Myriam Freund for assisting with French text translations; Steve Thurston (AMNH) for assistance with photography; Pio Colmenares and Lou Sorkin (AMNH) for assistance with import/export logistics from the U.S.

Appendix A. Supplementary material

Supplementary data to this article can be found online at https://doi.org/10.1016/j.ympev.2021.107212.

References

Abramsky, Z., Brand, S., Rosenzweig, M., 1985. Geographical ecology of gerbilline rodents in sand dune habitats of Israel. J. Biogeogr. 363–372.
Alqahtani, A.R., Badry, A., 2020. Interspecific phylogenetic relationship among different species of the genus *Buthacus* (Scorpiones: Buthidae) inferred from 16S rRNA in Egypt and Saudi Arabia. Zool. Middle East 66, 178–185.
Amr, Z.S., 2015. Scorpionism and dangerous species of Jordan. In: Gopalakrishnakone, P., Possani, L.D., Schwartz, E.F., de la Vega, R.C.R. (Eds.), Scorpion Venoms. Springer, Berlin, pp. 181–200.
Amr, Z.S., El-Oran, R., 1994. Systematics and distribution of scorpions (Arachnida, Scorpionida) in Jordan. Ital. J. Zool. 61, 185–190.
Amr, Z., Abed, O.A., Al Share, T., Hamidan, N., Prendini, L., 2015. New records of Jordanian scorpions. Jordan J. Nat. Hist. 2, 30–38.
Amr, Z.S., Hyland, K.E., Kinzelbach, R., Amr, S.S., Defosse, D., 1988. Scorpions et piqûres de scorpions en Jordanie. Bull. Soc. Pathol. Exot. 81, 369–379.
Badry, A., Younes, M., Sarhan, M.M.H., Saleh, M., 2018. On the scorpion fauna of Egypt, with an identification key (Arachnida: Scorpiones). Zool. Middle East 64, 75–87.
Barahoei, H., Prendini, L., Navidpour, S., Tahir, H.M., Aliabadian, M., Siahsarvie, R., Mirshamsi, O., 2021. Integrative systematics of the tooth-tailed scorpions, *Odontobuthus* (Buthidae), with descriptions of three new species from the Iranian Plateau. Zool. J. Linn. Soc. 2021, 1–43.
Bryson Jr., R.W., Prendini, L., Savary, W.E., Pearman, P.B., 2014. Caves as microrefugia: Pleistocene phylogeography of the troglophilic North American scorpion *Pseudouroctonus reddelli*. BMC Evol. Biol. 14, 9.
Bryson Jr., R.W., Riddle, B.R., Graham, M.R., Smith, B.T., Prendini, L., 2013a. As old as the hills: Montane scorpions in southwestern North America reveal ancient associations between biotic diversification and landscape history. PLoS ONE 8, e52822.
Bryson Jr., R.W., Savary, W.E., Prendini, L., 2013b. Biogeography of scorpions in the *Pseudouroctonus minimus* complex (Vaejovidae) from south-western North America: Implications of ecological specialization for pre-Quaternary diversification. J. Biogeogr. 40, 1850–1860.
Cain, S., Gefen, E., Prendini, L., 2021. Systematic revision of the sand scorpions, genus *Buthacus* Birula, 1908 (Buthidae C.L. Koch, 1837) of the Levant, with redescription of *Buthacus arenicola* (Simon, 1885) from Algeria and Tunisia. Bull. Am. Mus. Nat. Hist. 450, 1–134.
Cock, P.J.A., Antao, T., Chang, J.T., Chapman, B.A., Cox, C.J., Dalke, A., Friedberg, I., Hamelryck, T., Kauff, F., Wilczynski, B., De Hoon, M.J.L., 2009. Biopython: Freely

available Python tools for computational molecular biology and bioinformatics. Bioinformatics 25, 1422–1423.
Darriba, D., Taboada, G.L., Doallo, R., Posada, D., 2012. jModelTest 2: More models, new heuristics and parallel computing. Nat. Methods 9, 772.
Dimitrov, D., Astrin, J.J., Huber, B.A., 2013. Pholcid spider molecular systematics revisited, with new insights into the biogeography and the evolution of the group. Cladistics 29, 132–146.
Dimitrov, D., Lopardo, L., Giribet, G., Arnedo, M.A., Álvarez-Padilla, F., Hormiga, G., 2012. Tangled in a sparse spider web: Single origin of orb weavers and their spinning work unravelled by denser taxonomic sampling. Proc. R. Soc. B Biol. Sci. 279, 1341–1350.
Drummond, A.J., Suchard, M.A., Xie, D., Rambaut, A., 2012. Bayesian phylogenetics with BEAUti and the BEAST 1.7. Mol. Biol. Evol. 29, 1969–1973.
El-Hennawy, H.K., 1987. A simplified key to Egyptian scorpion species (Arachnida: Scorpionida). Serket 1, 15–17.
El-Hennawy, H.K., 1992. A catalogue of the scorpions described from the Arab countries (1758–1990) (Arachnida: Scorpionida). Serket 2, 95–153.
Esposito, L.A., Yamaguti, H.Y., Pinto-da-Rocha, R., Prendini, L., 2018. Plucking with the plectrum: Phylogeny of the New World buthid scorpion subfamily Centruroidinae Kraus, 1955 (Scorpiones: Buthidae) reveals evolution of three pecten-sternite stridulation organs. Arthropod Syst. Phylogeny 76, 87–122.
Fet, V., Lowe, G., 2000. Family Buthidae C.L. Koch, 1837. In: Catalog of the Scorpions of the World (1758–1998). The New York Entomological. Society, New York, pp. 54–286.
Fet, V., Gantenbein, B., Gromov, A.V., Lowe, G., Lourenço, W.R., 2003. The first molecular phylogeny of Buthidae (Scorpiones). Euscorpius 4, 1–10.
Ficetola, G.F., Mazel, F., Thuiller, W., 2017. Global determinants of zoogeographical boundaries. Nat. Ecol. Evol. 1, 1–7.
Fitch, W.M., 1971. Toward defining the course of evolution: Minimum change for a specific tree topology. Syst. Biol. 20, 406–416.
Fujita, M.K., Papenfuss, T.J., 2011. Molecular systematics of *Stenodactylus* (Gekkonidae), an Afro-Arabian gecko species complex. Mol. Phylogenet. Evol. 58, 71–75.
Gantenbein, B., Fet, V., Gantenbein-Ritter, I.A., Balloux, F., 2005. Evidence for recombination in scorpion mitochondrial DNA (Scorpiones: Buthidae). Proc. R. Soc. B Biol. Sci. 272, 697–704.
Gantenbein, B., Largiadèr, C.R., 2002. *Mesobuthus gibbosus* (Scorpiones: Buthidae) on the island of Rhodes—hybridization between Ulysses' stowaways and native scorpions? Mol. Ecol. 11, 925–938.
Georgalis, G.L., Gawad, M.K.A., Hassan, S.M., El-Barkooky, A.N., Hamdan, M.A., 2020. Oldest co-occurrence of *Varanus* and *Python* from Africa—first record of squamates from the early Miocene of Moghra Formation, Western Desert. Egypt. PeerJ 8, e9092.
Goloboff, P.A., Farris, J.S., Nixon, K.C., 2008. TNT, a free program for phylogenetic analysis. Cladistics 24, 774–786.
Goloboff, P.A., Farris, J.S., Nixon, K.C., 2003. T.N.T. Tree Analysis Using New Technology. Program and documentation available from the authors and at www.zmuc.dk/public/phylogeny.
Goloboff, P.A., Mattoni, C.I., Quinteros, A.S., 2006. Continuous characters analyzed as such. Cladistics 22, 589–601.
González-Santillán, E., Prendini, L., 2015. Phylogeny of the North American vaejovid scorpion subfamily Syntropinae Kraepelin, 1905, based on morphology, mitochondrial and nuclear DNA. Cladistics 31, 341–405.
Graham, M.R., Jaeger, J.R., Prendini, L., Riddle, B.R., 2013a. Phylogeography of the Arizona hairy scorpion (*Hadrurus arizonensis*) supports a model of biotic assembly in the Mojave Desert and adds a new Pleistocene refugium. J. Biogeogr. 40, 1298–1312.
Graham, M.R., Jaeger, J.R., Prendini, L., Riddle, B.R., 2013b. Phylogeography of Beck's desert scorpion, *Paruroctonus becki*, reveals Pliocene diversification in the eastern California Shear Zone and postglacial expansion in the Great Basin Desert. Mol. Phylogenet. Evol. 69, 502–513.
Graham, M.R., Myers, E.A., Kaiser, R.C., Fet, V., 2019. Cryptic species and co-diversification in sand scorpions from the Karakum and Kyzylkum deserts of Central Asia. Zool. Scr. 48, 801–812.
Graham, M.R., Stoev, P., Akkari, N., Blagoev, G., Fet, V., 2012. *Euscorpius sicanus* (Scorpiones: Euscorpiidae) from Tunisia: DNA barcoding confirms ancient disjunctions across the Mediterranean Sea. Serket 13, 16–26.
Graham, M.R., Wood, D.A., Henault, J.A., Valois, Z.J., Cushing, P.E., 2017. Ancient lakes, Pleistocene climates and river avulsions structure the phylogeography of a large but little-known rock scorpion from the Mojave and Sonoran deserts. Biol. J. Linn. Soc. 122, 133–146.
Grossman, A., Calvo, R., López-Antoñanzas, R., Knoll, F., Hartman, G., Rabinovich, R., 2019. First record of *Sivameryx* (Cetartiodactyla, Anthracotheriidae) from the lower Miocene of Israel highlights the importance of the Levantine Corridor as a dispersal route between Eurasia and Africa. J. Vertebr. Paleontol. 39, e1599901.
Guindon, S., Gascuel, O., 2003. A simple, fast, and accurate algorithm to estimate large phylogenies by maximum likelihood. Syst. Biol. 52, 696–704.
Harzhauser, M., Kroh, A., Mandic, O., Piller, W.E., Göhlich, U., Reuter, M., Berning, B., 2007. Biogeographic responses to geodynamics: A key study all around the Oligo-Miocene Tethyan Seaway. Zool. Anz. 246, 241–256.
Horowitz, A., 1988. The Quaternary environments and paleogeography in Israel. In: Yom-Tov, Y., Tchernov, E. (Eds.), The Zoogeography of Israel. Dr. W. Junk, Boston, pp. 35–57.
Hou, Z., Li, S., 2018. Tethyan changes shaped aquatic diversification. Biol. Rev. 93, 874–896.
International Union for the Conservation of Nature (IUCN), 2019. The IUCN Red List of Threatened Species. Version 2019-2. Available at http://www.iucnredlist.org (accessed 7.10.19).
Kabakibi, M.M., Khalil, N., Amr, Z., 1999. Scorpions of southern Syria. Zool. Middle East 17, 79–89.
Kapli, P., Lymberakis, P., Crochet, P.-A., Geniez, P., Brito, J.C., Almutairi, M., Ahmadzadeh, F., Schmitz, A., Wilms, T., Pouyani, N.R., Poulakakis, N., 2015. Historical biogeography of the lacertid lizard *Mesalina* in North Africa and the Middle East. J. Biogeogr. 42, 267–279.
Kovařík, F., 2001. Catalog of the Scorpions of the World (1758–1998) by V. Fet, W.D. Sissom, G. Lowe, and M. Braunwalder (New York Entomological Society, 2000: 690 pp.). Discussion and supplement for 1999 and part of 2000. Serket 7, 78–93.
Kovařík, F., 2018. Notes on the genera *Buthacus*, *Compsobuthus*, and *Lanzatus* with several synonymies and corrections of published characters (Scorpiones: Buthidae). Euscorpius 269, 1–12.
Kovařík, F., 2005. Taxonomic position of species of the genus *Buthacus* Birula, 1908 described by Ehrenberg and Lourenço, and description of a new species (Scorpiones: Buthidae). Euscorpius 28, 1–13.
Kovařík, F., Lowe, G., Plíšková, J., Šťáhlavský, F., 2013. A new scorpion genus, *Gint* gen. n., from the Horn of Africa (Scorpiones: Buthidae). Euscorpius 173, 1–19.
Kovařík, F., Lowe, G., Šťáhlavský, F., 2016. Review of northwestern African *Buthacus*, with description of *Buthacus stockmanni* sp. n. from Morocco and Western Sahara (Scorpiones, Buthidae). Euscorpius 236, 1–18.
Kovarik, F., Whitman, S., 2004. Cataloghi del Museo di Storia Naturale dell'Università di Firenze—sezione di zoologia «La Specola» XXII. Arachnida Scorpiones. Tipi. Addenda (1998–2004) e checklist della collezione (Euscorpiinae esclusi). Atti Soc. Toscana Sci. Nat. Mem. Ser. B 111, 103–119.
Kugler, J., 1988. Zoogeography of social insects of Israel and Sinai. In: Yom-Tov, Y., Tchernov, E. (Eds.), The Zoogeography of Israel. Dr. W. Junk Publishers, Boston, pp. 251–275.
Kumar, S., Stecher, G., Li, M., Knyaz, C., Tamura, K., 2018. MEGA X: Molecular Evolutionary Genetics Analysis across computing platforms. Mol. Biol. Evol. 35, 1547–1549.
Leprieur, F., Descombes, P., Gaboriau, T., Cowman, P.F., Parravicini, V., Kulbicki, M., Melián, C.J., De Santana, C.N., Heine, C., Mouillot, D., Bellwood, D.R., Pellissier, L., 2016. Plate tectonics drive tropical reef biodiversity dynamics. Nat. Commun. 7, 1–8.
Levy, G., Amitai, P., 1980. Fauna Palaestina. Arachnida. I. Scorpiones. Israel Academy of Sciences and Humanities, Jerusalem.
Levy, G., Amitai, P., Shulov, A., 1973. New scorpions from Israel, Jordan and Arabia. Zool. J. Linn. Soc. 52, 113–140.
Lewis, P.O., 2001. A likelihood approach to estimating phylogeny from discrete morphological character data. Syst. Biol. 50, 913–925.
López-Antoñanzas, R., Gutkin, V., Rabinovich, R., Calvo, R., Grossman, A., 2016. A transitional gundi (Rodentia: Ctenodactylidae) from the Miocene of Israel. PLoS ONE 11, e0151804.
López-Antoñanzas, R., Renaud, S., Peláez-Campomanes, P., Azar, D., Kachacha, G., Knoll, F., 2019. First levantine fossil murines shed new light on the earliest intercontinental dispersal of mice. Sci. Rep. 9, 11874.
Lourenço, W.R., 2006. Further considerations on the genus *Buthacus* Birula, 1908. Bol. Soc. Entomol. Aragon. 1, 59–70.
Lourenço, W.R., 2004. Description of a new species of *Buthacus* Birula (Scorpiones, Buthidae) from Afghanistan. Entomol. Mitt. Zool. Mus. Hamburg 14, 205–210.
Lourenço, W.R., Qi, J.-X., 2006. A new species of the genus *Buthacus* Birula, 1908 (Scorpiones, Buthidae), from Pakistan. Bol. Soc. Entomol. Aragon. 39, 161–164.
Lourenço, W.R., Sadine, S.E., 2015. A new species of *Buthacus* Birula, 1908 from the region of Ghardaïa, Algeria (Scorpiones, Buthidae). Rev. Ibér. Aracnol. 27, 55–59.
Lowe, G., Kovařík, F., Stockmann, M., Šťáhlavský, F., 2019. *Trypanothacus* gen. n., a new genus of burrowing scorpion from the Arabian Peninsula (Scorpiones: Buthidae). Euscorpius 277, 1–30.
Machado, L., Salvi, D., Harris, D.J., Brito, J.C., Crochet, P.-A., Geniez, P., Ahmadzadeh, F., Carranza, S., 2020. Systematics, biogeography and evolution of the Saharo-Arabian naked-toed geckos genus *Tropiocolotes*. Mol. Phylogenet. Evol. https://doi.org/10.1016/j.ympev.2020.106969.
Maddison, W.P., Maddison, D.R., 2019. Mesquite: A modular system for evolutionary analysis. Version 3.5. Available at http://www.mesquiteproject.org.
Matzke, N.J., 2014. Model selection in historical biogeography reveals that founder-event speciation is a crucial process in island clades. Syst. Biol. 63, 951–970.
Matzke, N.J., 2013a. BioGeoBEARS: BioGeography with Bayesian (and Likelihood) Evolutionary Analysis in R Scripts. R Package. Version 0.2.1. Available at http://CRAN.R-project.org/package=BioGeoBEARS.
Matzke, N.J., 2013b. Probabilistic historical biogeography: New models for founder-event speciation, imperfect detection, and fossils allow improved accuracy and model-testing. Front. Biogeogr. 5, 242–248.
Miller, M.A., Pfeiffer, W., Schwartz, T., 2010. Creating the CIPRES Science Gateway for inference of large phylogenetic trees, in: Gateway Computing Environments Workshop (GCE). New Orleans, LA, pp. 1–8.
Nixon, K.C., 2002. WinClada, ver. 1.00.08. Computer software and documentation. Available at http://www.diversityoflife.org/winclada.
Paradis, E., Claude, J., Strimmer, K., 2004. APE: Analyses of Phylogenetics and Evolution in R language. Bioinformatics 20, 289–290.
Pellissier, L., Heine, C., Rosauer, D.F., Albouy, C., 2018. Are global hotspots of endemic richness shaped by plate tectonics? Biol. J. Linn. Soc. 123, 247–261.
Polis, G.A., Myers, C., Quinlan, M., 1986. Burrowing biology and spatial distribution of desert scorpions. J. Arid Environ. 10, 137–146.

Pook, C.E., Joger, U., Stümpel, N., Wüster, W., 2009. When continents collide: Phylogeny, historical biogeography and systematics of the medically important viper genus *Echis* (Squamata: Serpentes: Viperidae). Mol. Phylogenet. Evol. 53, 792–807.
Prendini, L., 2001a. Substratum specialization and speciation in southern African scorpions: The Effect Hypothesis revisited. In: Fet, V., Selden, P.A. (Eds.), Scorpions 2001. In Memoriam Gary A. Polis. British Arachnological Society, Burnham Beeches, UK, pp. 113–139.
Prendini, L., 2001b. Phylogeny of *Parabuthus* (Scorpiones, Buthidae). Zool. Scr. 30, 13–35.
Prendini, L., 2004. Systematics of the genus *Pseudolychas* Kraepelin (Scorpiones: Buthidae). Ann. Entomol. Soc. Am. 97, 37–63.
Prendini, L., Esposito, L.A., 2010. A reanalysis of *Parabuthus* (Scorpiones: Buthidae) phylogeny with descriptions of two new *Parabuthus* species endemic to the Central Namib gravel plains, Namibia. Zool. J. Linn. Soc. 159, 673–710.
Prendini, L., Crowe, T.M., Wheeler, W.C., 2003. Systematics and biogeography of the family Scorpionidae (Chelicerata: Scorpiones), with a discussion on phylogenetic methods. Invertebr. Syst. 17, 185–259.
Prendini, L., Hanner, R., DeSalle, R., 2002. Obtaining, storing and archiving specimens and tissue samples for use in molecular studies. In: DeSalle, R., Giribet, G., Wheeler, W.C. (Eds.), Techniques in Molecular Systematics and Evolution. Birkhäuser Verlag AG, Basel, pp. 176–248.
Prendini, L., Weygoldt, P., Wheeler, W.C., 2005. Systematics of the *Damon variegatus* group of African whip spiders (Chelicerata: Amblypygi): Evidence from behaviour, morphology and DNA. Org. Divers. Evol. 5, 203–236.
Rambaut, A., Suchard, M.A., Xie, D., Drummond, A.J., 2014. Tracer 1.6. Available at http://beast.bio.ed.ac.uk/tracer.
Revell, L.J., 2012. phytools: An R package for phylogenetic comparative biology (and other things). Methods Ecol. Evol. 3, 217–223.
Rögl, F., 1999. Mediterranean and Paratethys. Facts and hypotheses of an Oligocene to Miocene Paleogeography (short overview). Geol. Carpathica 50, 339–349.
Ronquist, F., Huelsenbeck, J.P., 2003. MrBayes 3: Bayesian phylogenetic inference under mixed models. Bioinformatics 19, 1572–1574.
Saleh, M., Younes, M., Badry, A., Sarhan, M., 2017. Zoogeographical analysis of the Egyptian scorpion fauna. Al-Azhar Bull. Sci. 28, 1–14.
Santibáñez-López, C.E., Francke, O.F., Prendini, L., 2014. Phylogeny of the North American scorpion genus *Diplocentrus* Peters, 1861 (Scorpiones: Diplocentridae) based on morphology, nuclear and mitochondrial DNA. Arthropod Syst. Phylogeny 72, 257–279.
Sen, S., 2013. Dispersal of African mammals in Eurasia during the Cenozoic: Ways and whys. Geobios 46, 159–172.
Shehab, A.H., Amr, Z.S., Lindsell, J.A., 2011. Ecology and biology of scorpions in Palmyra, Syria. Turkish J. Zool. 35, 333–341.
Singer, A., 2007. The soils of Israel. Springer, Berlin.
Stahnke, E.L., 1972. UV light, a useful field tool. Bioscience 22, 604–607.
Stamatakis, A., 2014. RAxML version 8: A tool for phylogenetic analysis and post-analysis of large phylogenies. Bioinformatics 30, 1312–1313.
Stamatakis, A., 2006. RAxML-VI-HPC: Maximum likelihood-based phylogenetic analyses with thousands of taxa and mixed models. Bioinformatics 22, 2688–2690.
Stecher, G., Tamura, K., Kumar, S., 2020. Molecular Evolutionary Genetics Analysis (MEGA) for macOS. Mol. Biol. Evol. 37, 1237–1239.
Suranse, V., Sawant, N.S., Paripatyadar, S.V., Krutha, K., Paingankar, M.S., Padhye, A.D., Bastawade, D.B., Dahanukar, N., 2017. First molecular phylogeny of scorpions of the family Buthidae from India. Mitochondrial DNA 28, 606–611.
Talal, S., Tesler, I., Sivan, J., Ben-Shlomo, R., Tahir, H.M., Prendini, L., Snir, S., Gefen, E., 2015. Scorpion speciation in the Holy Land: Multilocus phylogeography corroborates diagnostic differences in morphology and burrowing behavior among *Scorpio* subspecies and justifies recognition as phylogenetic, ecological and biological species. Mol. Phylogenet. Evol. 91, 226–237.
Tamura, K., Nei, M., Kumar, S., 2004. Prospects for inferring very large phylogenies by using the neighbor-joining method. Proc. Natl. Acad. Sci., U.S.A. 101, 11030–11035.
Tamura, K., Stecher, G., Peterson, D., Filipski, A., Kumar, S., 2013. MEGA6: Molecular Evolutionary Genetics Analysis version 6.0. Mol. Biol. Evol. 30, 2725–2729.
Tchernov, E., 1988. The biogeographical history of the southern Levant. In: Yom-Tov, Y., Tchernov, E. (Eds.), The Zoogeography of Israel. Dr. W. Junk, Boston, pp. 159–250.
Vachon, M., 1952. Etudes sur les scorpions. Institut Pasteur d'Algérie, Algiers.
Vachon, M., Kinzelbach, R., 1987. On the taxonomy and distribution of the scorpions of the Middle East. In: Krupp, F., Schneider, W., Kinzelbach, R. (Eds.), Proceedings of the Symposium on the Fauna and Zoogeography of the Middle East, Mainz, 1985. Beihefte zum Tübinger Atlas des Vorderen Orients (TAVO), Reihe A (Naturwissenschaften), pp. 91–103.
Werner, Y.L., 1988. Herpetofaunal survey of Israel (1950–85), with comments on Sinai and Jordan and on zoogeographical heterogeneity. In: Yom-Tov, Y., Tchernov, E. (Eds.), The Zoogeography of Israel. Dr. W. Junk, Boston, pp. 355–387.
Werner, Y.L., Le Verdier, A., Rosenman, D., Sivan, N., 1991. Systematics and zoogeography of *Cerastes* (Ophidia: Viperidae) in the Levant: 1, Distinguishing Arabian from African "*Cerastes cerastes*". The Snake 23, 90–100.
Wiemers, M., Keller, A., Wolf, M., 2009. ITS2 secondary structure improves phylogeny estimation in a radiation of blue butterflies of the subgenus *Agrodiaetus* (Lepidoptera: Lycaenidae: Polyommatus). BMC Evol. Biol. 9 https://doi.org/10.1186/1471-2148-9-300.
Wilson, J.D., Raven, R.J., Schmidt, D.J., Hughes, J.M., Rix, M.G., 2020. Total-evidence analysis of an undescribed fauna: Resolving the evolution and classification of Australia's golden trapdoor spiders (Idiopidae: Arbanitinae: Euoplini). Cladistics 36, 543–568.
Yağmur, E.A., Yalçın, M., Çalışır, G., 2008. Distribution of *Androctonus crassicauda* (Olivier 1807) and *Buthacus macrocentrus* (Ehrenberg 1828) (Scorpiones: Buthidae) in Turkey. Serket 11, 13–18.
Zaffos, A., Finnegan, S., Peters, S.E., 2017. Plate tectonic regulation of global marine animal diversity. Proc. Natl. Acad. Sci., U.S.A. 114, 5653–5658.
Zambre, A.M., Lourenço, W.R., 2010. A new species of *Buthacus* Birula, 1908 (Scorpiones, Buthidae) from India. Bol. Soc. Entomol. Aragon. 46, 115–119.